

# Particle identification with the cluster counting technique

Federica Cuna for the cluster counting team



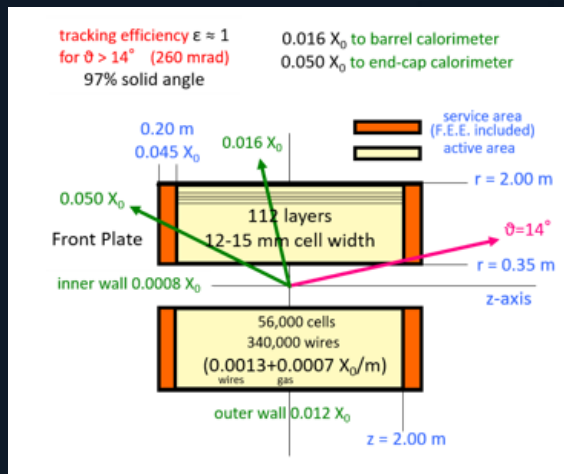
# Outline

---

- The IDEA drift chamber: an innovative tracker with high particle identification potential
- The cluster counting technique: a promising method for the particle identification
- The simulations results with Garfield++ and Geant4: first hint of great results
- Beam tests for the validation of the great expectations

## The IDEA drift chamber

The IDEA drift chamber (DCH) is the tracker of FCC-ee and CEPC. It is designed to provide efficient tracking, high precision momentum measurement and excellent particle identification by exploiting the application of the **cluster counting technique**.



- He based gas mixture (90% He – 10% i-C<sub>4</sub>H<sub>10</sub>)
- Full stereo configuration with alternating sign stereo angles ranging from 50 to 250 mrad
- 12 ÷ 14.5 mm wide square cells 5 : 1 field to sense wires ratio
- 56,448 cells
- 14 co-axial super-layers, 8 layers each (112 total) in 24 equal azimuthal (15°) sectors

- **Gas containment – wire support functions separation:**

the total amount of material in radial direction, towards the barrel calorimeter, is of the order of 1.6%  $X_0$ , whereas in the forward and backward directions it is equivalent to about 5.0%  $X_0$ , including the endplates instrumented with front end electronics.

- **Cluster timing:**

allows to reach spatial resolution  $< 100 \mu\text{m}$  for 8 mm drift cells in He based gas mixtures (such a technique is going to be implemented in the MEG-II drift chamber under construction)

- **Cluster counting:**

allows to reach  $dN/dx$  resolution  $< 3\%$  for particle identification (a factor 2 better than  $dE/dx$ )

# The cluster counting technique

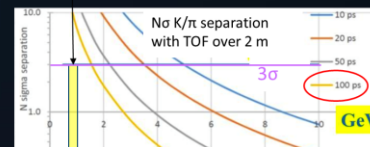
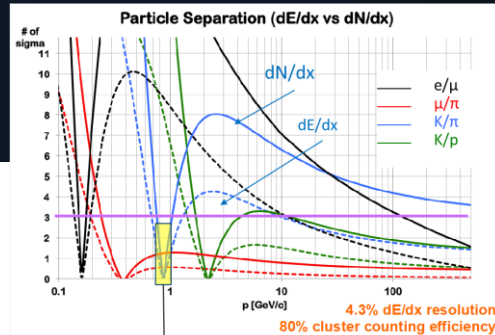
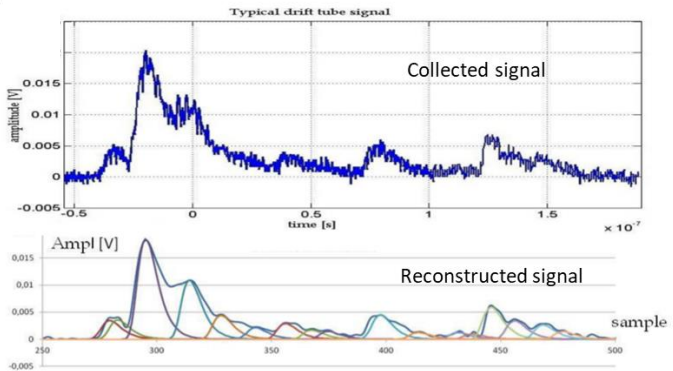
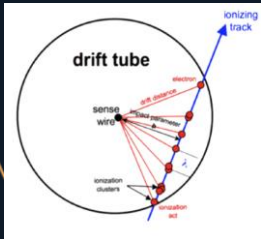
## The traditional technique: $dE/dx$

Using the information about energy deposit by a track in a gaseous detector, particle identification can be performed.

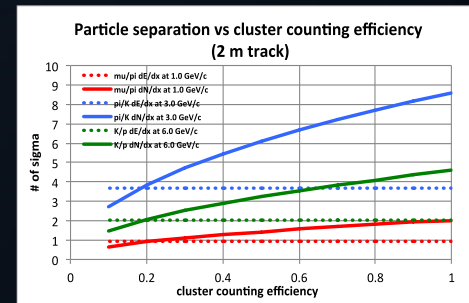
The large and intrinsic uncertainties in the total energy deposition represent a limit to the particle separation capabilities.

## The cluster counting technique : $dN/dx$

The method consists in singling out, in ever recorded detector signal, the isolated structures related to the arrival on the anode wire of the electrons belonging to a single ionization act.



Analytical evaluation  
by F. Grancagnolo



80% cluster counting efficiency.

Expected excellent  $K/\pi$  separation over the entire range except  $0.85 < p < 1.05$  GeV (blue lines)

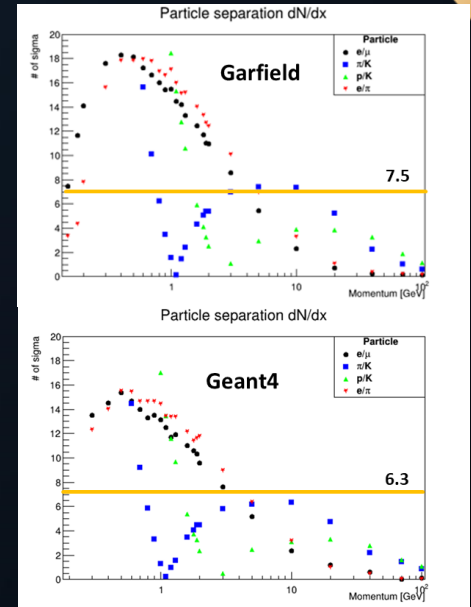
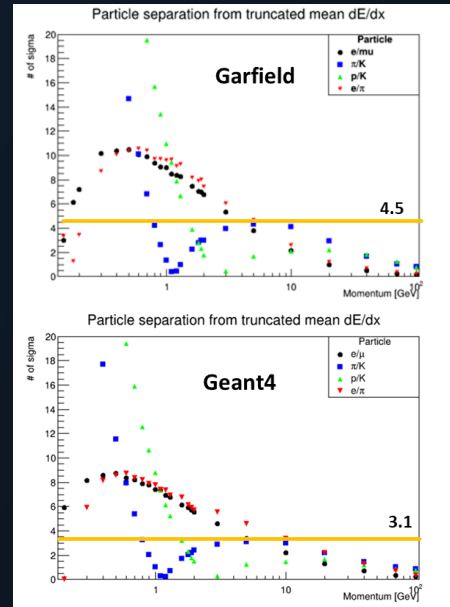
Could recover with timing layer

# Simulation results with Garfield++ and Geant4

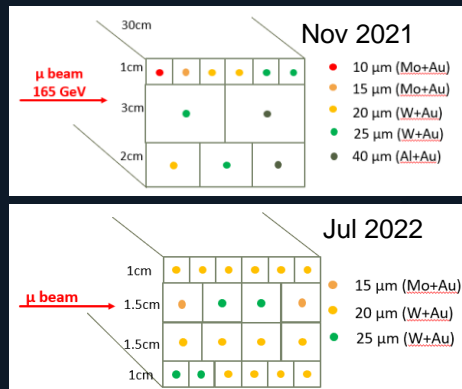
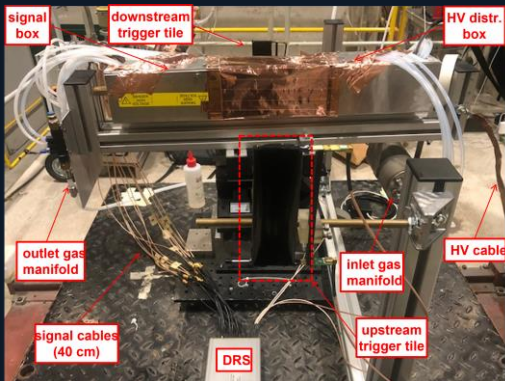
A simulation of the ionization process in 1 cm long side cell of 90% He and 10%  $iC_4H_{10}$  has been performed in **Garfield++** and **Geant4**.

Three different algorithms have been implemented to simulate in **Geant4**, *in a fast and convenient way*, the number of clusters and clusters size distributions, using the energy deposit provided by **Geant4**.

The simulations confirm the predictions: a factor 2 better than  $dE/dx$  !

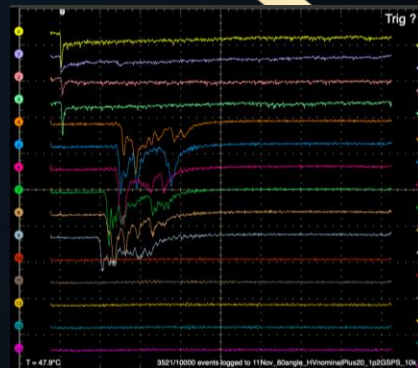


# Beam tests to validate the simulations results



## A "minimal" setup

- A pack of drift tubes
- DRS for data acquisition
- Gas mixing, control and distribution (He and  $\text{iC}_4\text{H}_{10}$ )
- 2 trigger scintillators

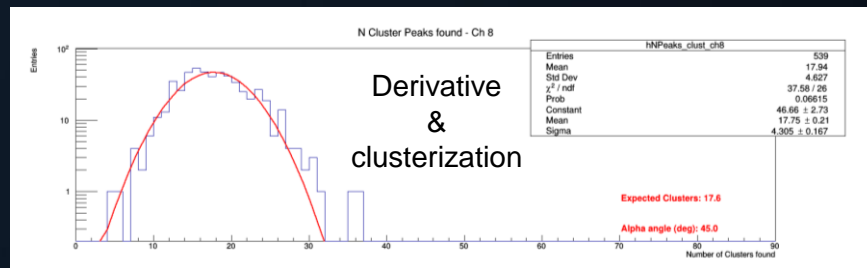


Two algorithms for peaks finding:

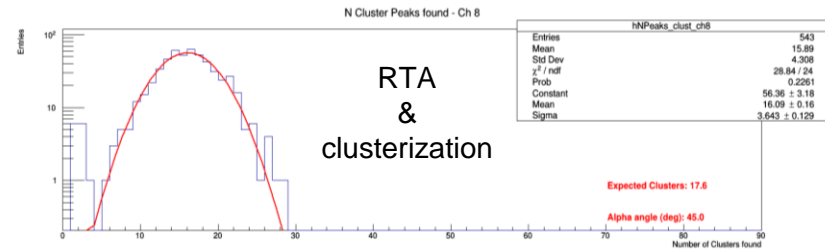
- Derivative algorithm
- Running template algorithm (RTA)

An algorithm to associate the peaks found in clusters:

- Clusterization algorithm



Poissonian nature



# Thank you

## The cluster counting team

C. Caputo<sup>1</sup>, G. Chiarello<sup>2</sup>, A. Corvaglia<sup>3</sup>, F. Cuna<sup>2,3</sup>, B. D'Anzi<sup>4,5</sup>, N. De Filippis<sup>5,6</sup>, F. De Santis<sup>2,3</sup>, W. Elmetenawee<sup>5</sup>, E. Gorini<sup>2</sup>, F. Grancagnolo<sup>2</sup>, M. Greco<sup>2,3</sup>, S. Griбанov, K. Johnson<sup>7</sup>, M. Louka<sup>4,5</sup>, P. Mastrapsqua<sup>1</sup>, A. Miccoli<sup>2</sup>, M. Panareo<sup>2</sup>, A. Popov, M. Primavera<sup>2</sup>, A. Taliercio<sup>9</sup>, G. F. Tassielli<sup>4</sup>, A. Ventura<sup>2</sup>, S. Xin<sup>8</sup>, Fangyi Guo<sup>8</sup>, Shuaiyi Liu<sup>8</sup>

<sup>1</sup>Université Catholique de Louvain, Belgium, <sup>2</sup>Istituto Nazionale di Fisica Nucleare, Lecce, Italy, <sup>3</sup>Università del Salento, Italy, <sup>4</sup>Università degli Studi di Bari »Aldo Moro«, Italy, <sup>5</sup>Istituto Nazionale di Fisica Nucleare, Bari, Italy, <sup>6</sup>Politecnico di Bari, <sup>7</sup>Florida State University, <sup>8</sup>Institute of High energy Physics, <sup>9</sup>Northwestern University, Illinois

The background is a dark blue gradient. There are several gold-colored decorative elements: a thick arc in the top-left corner, a thin arc in the bottom-right corner, and a thin horizontal line underlining the word 'Backup'.

# Backup

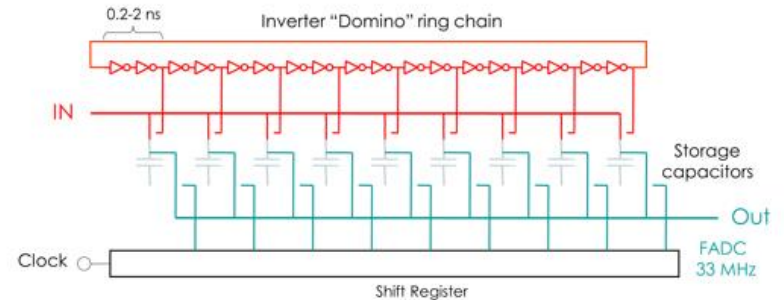


## The DAQ system: WDB wave dream board

Special thanks to the MEG collaboration

16 ch Drs4 REAdout Module

16 channels data acquisition board designed and used by the MEG2 experiment at PSI ( $\mu \rightarrow e + \gamma$ )



- **Analog switched capacitor array:** analog memory with a depth of 1024 sampling cells, perform a “**sliding window**” sampling.
- **500MSPS ↔ 5GSPS sampling speed** with 11.5 bit signal-noise ratio
  - 8 analog channels + 1 clock-dedicated channel for sub 50ps time alignment
- Pile-up rejection  $O(\sim 10 \text{ ns})$
- Time measurement  $O(10 \text{ ps})$
- Charge measurement  $O(0.1\%)$

The data files have been converted in root format to accomplish the data analysis.

Data at different configuration have been collected:

- 90%He-10%iC<sub>4</sub>H<sub>10</sub>
- 80%He-20%iC<sub>4</sub>H<sub>10</sub>
- HV nominal (+10,+20,+30,-10,-20,-30)
- Angle 0°, 30°, 45°, 60°

Details at: Application of the DRS chip for fast waveform digitizing, Stefan Ritt, Roberto Dinapoli, Ueli Hartmann, *Nuclear Instruments and Methods in Physics Research A* 623 (2010) 486–488

## The DAQ system: an oscilloscope interface

WDB interface is similar to the interface of an oscilloscope with 16 channels

The image displays the WDB DAQ system interface, which functions as a 16-channel oscilloscope. The main display shows multiple colored waveforms corresponding to different channels. Annotations on the left side of the interface indicate channel groupings:
 

- 4 trigger channels (channels 0-3)
- 6 tubes 1 cm cell size with typical event (channels 4-9)
- 3 tubes 2 cm cell size (channels 10-12)
- 2 tubes 3 cm cell size (channels 13-14)
- typical event (channel 15)

 The right side of the interface features several control panels:
 

- Channel selection panel:** A 4x4 grid of buttons labeled 0-15 for selecting individual channels.
- Trigger selection pattern:** A grid for defining trigger patterns across channels.
- Gain selection:** A control for setting the gain for each channel, currently set to 10.
- Channels setting table:** A detailed table for configuring each channel's gain, PZC, trigger level, HV, and current.

 The bottom right corner shows a table titled "Channels setting" with the following data:
 

Chn	Gain	PZC	Trigger Level	HV	Current
0	10	PZC	-19 mV	0 V	0 uA
1	10	PZC	-19 mV	0 V	0 uA
2	10	PZC	-19 mV	0 V	0 uA
3	10	PZC	-19 mV	0 V	0 uA
4	10	PZC	-19 mV	0 V	0 uA
5	10	PZC	-19 mV	0 V	0 uA
6	10	PZC	-19 mV	0 V	0 uA
7	10	PZC	-19 mV	0 V	0 uA
8	10	PZC	-19 mV	0 V	0 uA
9	10	PZC	-19 mV	0 V	0 uA
10	10	PZC	-19 mV	0 V	0 uA
11	10	PZC	-19 mV	0 V	0 uA
12	10	PZC	-19 mV	0 V	0 uA
13	10	PZC	-19 mV	0 V	0 uA
14	10	PZC	-19 mV	0 V	0 uA
15	10	PZC	-19 mV	0 V	0 uA

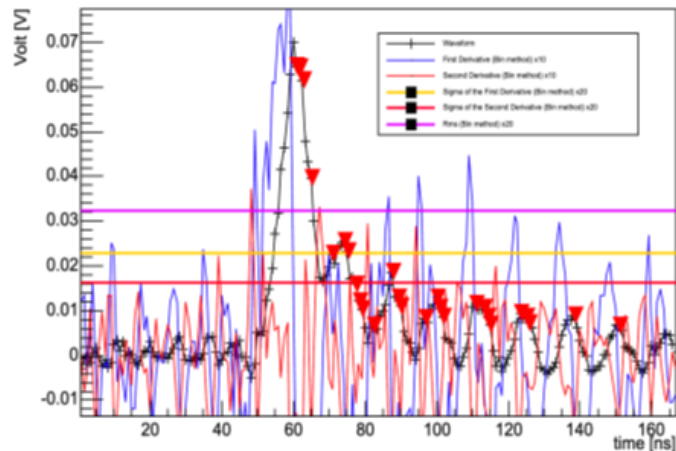
## Preliminary results: an efficient algorithm to count electrons

### The first and second derivative algorithm (DERIV)

Requirements for a good peak candidate in the bin position [ip]:

1. Amplitude constraint:
  - $\text{Amplitude[ip]} > 4 * \text{rms}$
  - $\text{Amplitude[ip]} - \text{Amplitude[ip-1]} > \text{rms} \ || \ \text{Amplitude[ip+1]} - \text{Amplitude[ip-1]} > \text{rms}$
2. First derivative constraint:
  - $\text{Fderiv[ip]} < \sigma_{\text{der1}}/2$
  - $\text{Fderiv[ip-1]} > \sigma_{\text{der1}} \ || \ \text{Fderiv[ip+1]} < \sigma_{\text{der1}}$
3. Second derivative constraint:
  - $\text{Sderiv[ip]} < 0$

0°, nominal HV+20, 90%He-10%iC<sub>4</sub>H<sub>10</sub>  
Tube with 1 cm cell size and 20 μm diameter

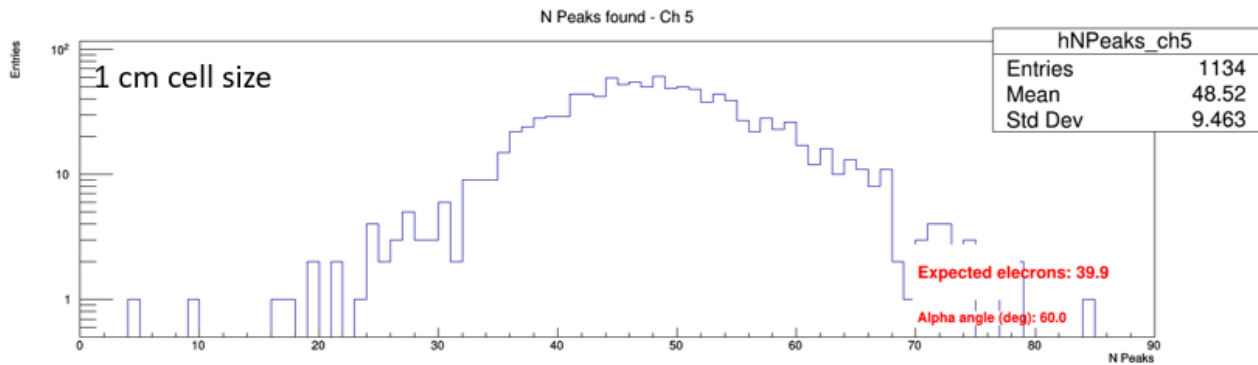


Expected number of electrons peaks:

$$N_{\text{peak}} = \delta_{\text{cluster/cm(M.I.P.)}} * \text{drift tube size [cm]} * 1.3 (\text{relativistic rise}) * 1.6 \text{ electron/cluster} * 1/\cos(\alpha)$$

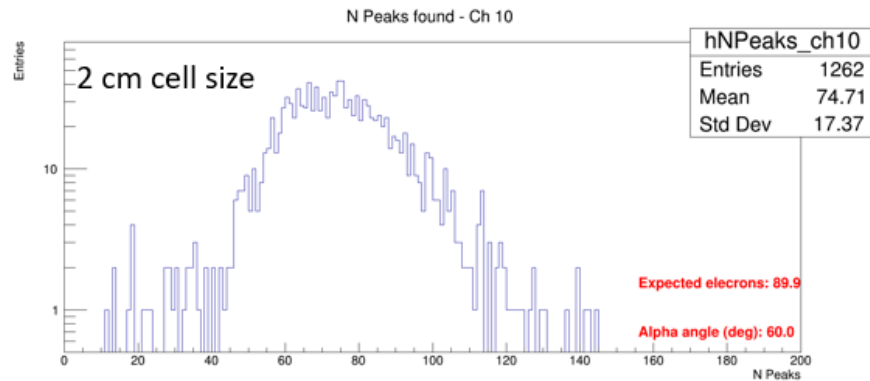
- $\delta_{\text{cluster/cm(M.I.P.)}}$  changes from 12 to 18 respectively for 90%He and 80%iC<sub>4</sub>H<sub>10</sub>
- Drift tube size changes from 0.8 to 1.8 respectively for 1 cm and 2 cm cell size tube.
- $\alpha$  is the angle of the muon tracks to the detector

## The first and second derivative algorithm: results



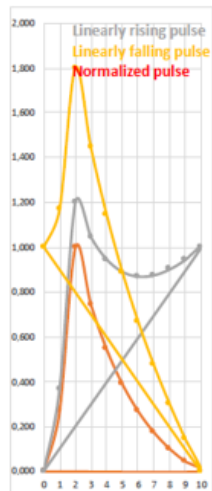
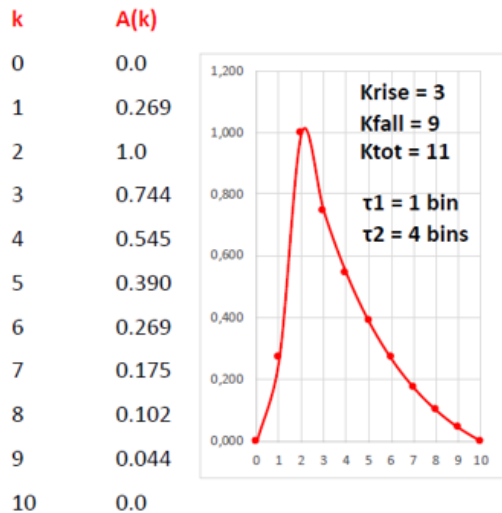
90%He-10%<sup>i</sup>C<sub>4</sub>H<sub>10</sub>  
60°  
nominal HV+20

The mean values are compatible with the ones expected!

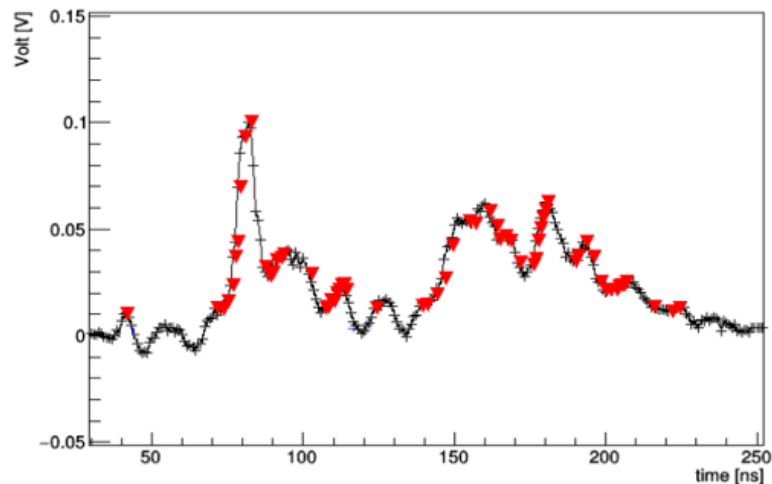


## The running template algorithm (RTA)

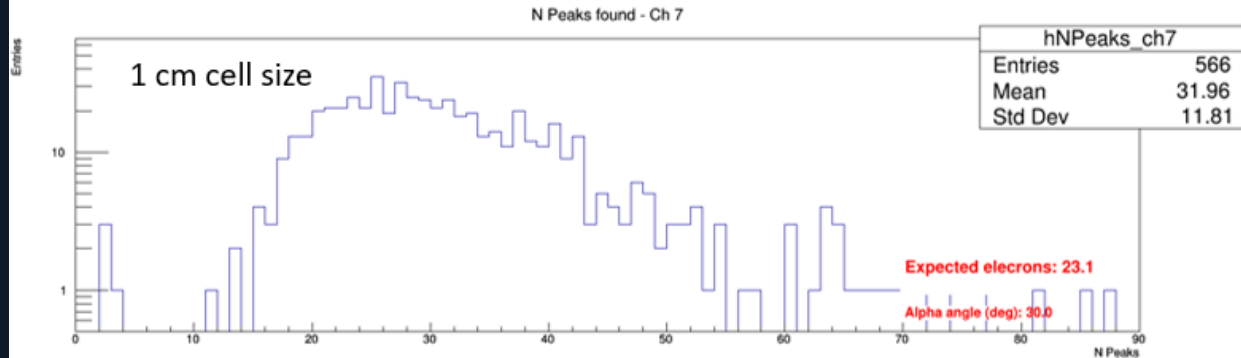
- Define an electron pulse template based on experimental data.
- Raising and falling exponential over a fixed number of bins ( $K_{tot}$ ).
- Digitize it ( $A(k)$ ) according to the data sampling rate.
- Run over  $K_{tot}$  bins by comparing it to the subtracted and normalized data (build a sort of  $\chi^2$ ).
- Define a cut on  $\chi^2$ .
- Subtract the found peak to the signal spectrum.
- Iterate the search.
- Stop when no new peak is found.



30°, nominal HV+20, 90%He-10%iC<sub>4</sub>H<sub>10</sub>  
Tube with 1 cm cell size and 20  $\mu$ m diameter

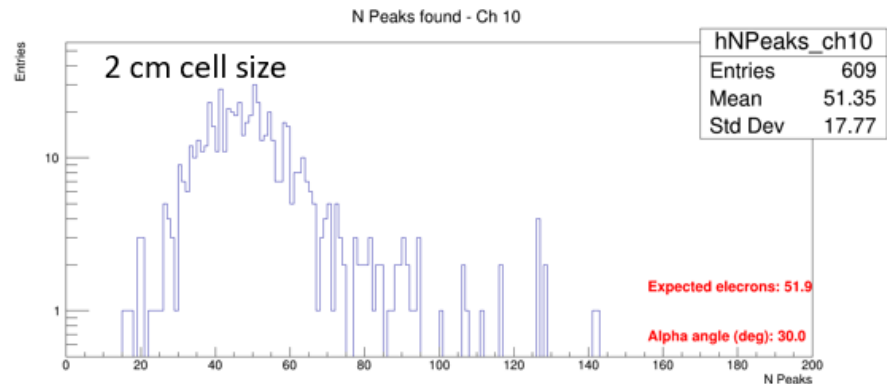


## The running template algorithm (RTA): results



90%He-10% $i$ C<sub>4</sub>H<sub>10</sub>  
30°  
nominal HV+20

The mean values are compatible with the ones expected!

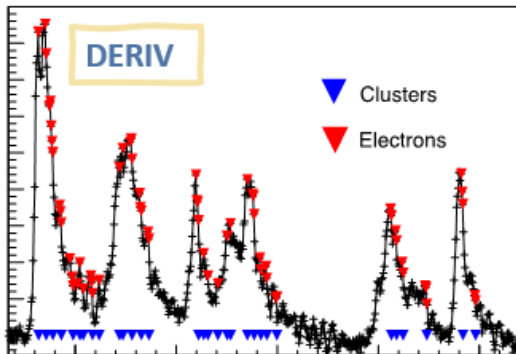


## A single clusterization algorithm

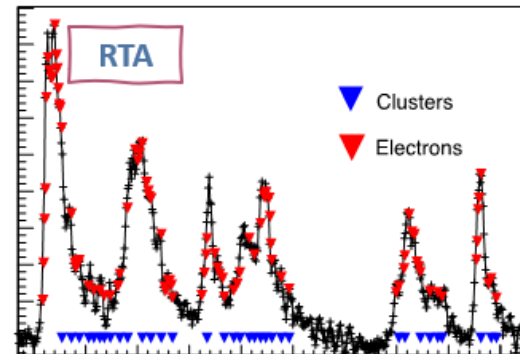
Once find the electron peaks, clusterization of the electron peaks into ionization clusters has been implemented:

- 1) Association of electron peaks consisting in consecutive bins (difference in time == 1 bin) electrons to a single electron in order to eliminate fake electrons.
- 2) Contiguous electrons peaks which are compatible with the electrons diffusion time (2.5 ns or 3 bins) must be considered belonging to the same ionization cluster.
- 3) Position of the clusters is taken as the position of the last electron in the cluster.

2 cm drift tube Track angle 45°



2 cm drift tube Track angle 45°



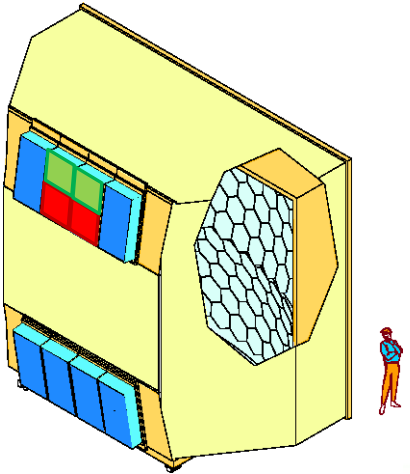
# SINGLE PHOTON DETECTION WITH MPGDS

Daniele D'Ago on behalf of COMPASS RICH group

Cover large area with photon detectors in COMPASS RICH ( $\sim 1.4 \text{ m}^2$ )

Why MPGDS?

- > Reduced ion and photon backflow to photocathode > reduced aging and improved electrical stability
- > Faster signal development > higher rate capabilities



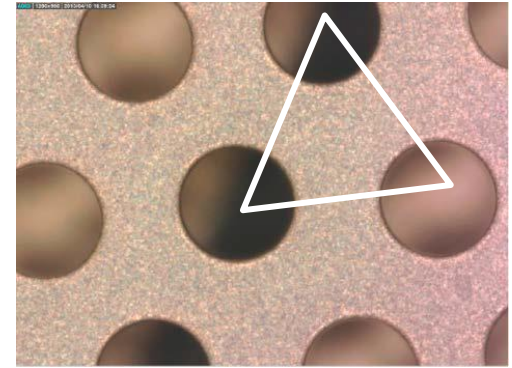
$600 \times 600 \text{ mm}^2$  Photon detectors  
composed of two equal segments

Fused silica window

2 layers of THGEM (staggered)  
first THGEM coated with CsI  
> reflective photocathode

1 Micromegas  
Suppresses ion backflow (3%)

Gas Mixture:  $\text{Ar} : \text{CH}_4 = 50 : 50$



Dielectric Thickness:  $400 \mu\text{m}$   
Hole  $\varnothing$ :  $400 \mu\text{m}$   
Hole in triangular pattern  
Hole pitch:  $800 \mu\text{m}$   
No rim

Bulk Micromegas  
Stainless steel, woven mesh  
Anodic distance:  $128 \mu\text{m}$   
Wire  $\varnothing$ :  $18 \mu\text{m}$   
Wire pitch:  $63 \mu\text{m}$

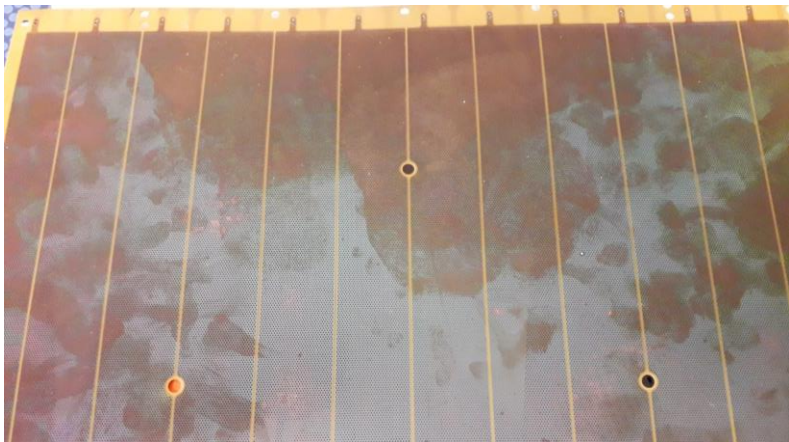


# POWERING AND READOUT

Electrode segmentation is essential. Each sector biased via  $500\text{ M}\Omega$  resistor.

- > discharges affect single sector
- > operating conditions restored in  $\sim 10\text{ s}$

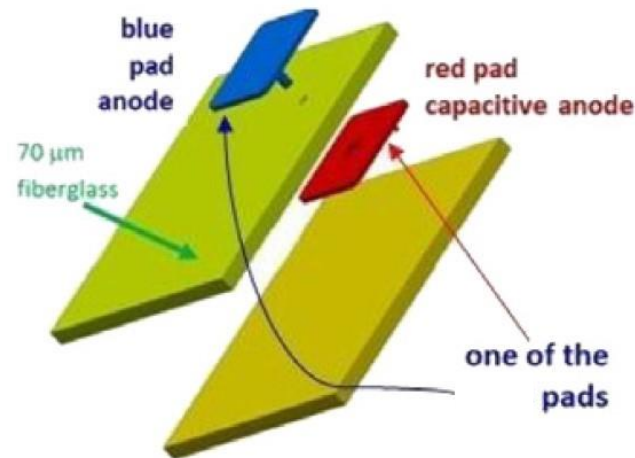
Voltages rescaled according to p and T fluctuations > stability of gain ( $\sim 6\%$ )



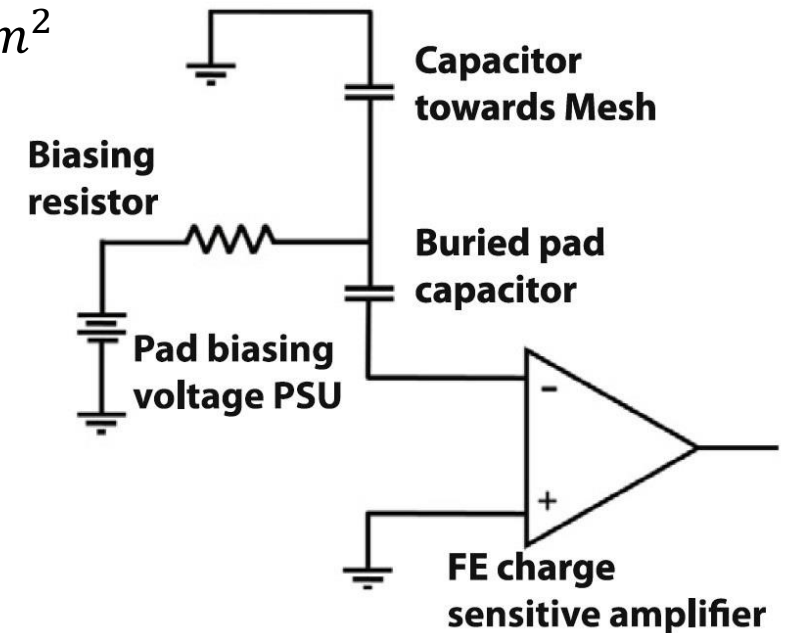
Large number of HV channels ( $\sim 100$ ) > compromise between cost and flexibility



Readout pad size:  $7.5 \times 7.5\text{ mm}^2$   
Readout pad pitch:  $8\text{ mm}$



“resistive” MM:  
 $470\text{ M}\Omega$  in series with each pad  
Signal collected by buried pad  
and read with APV25 chip



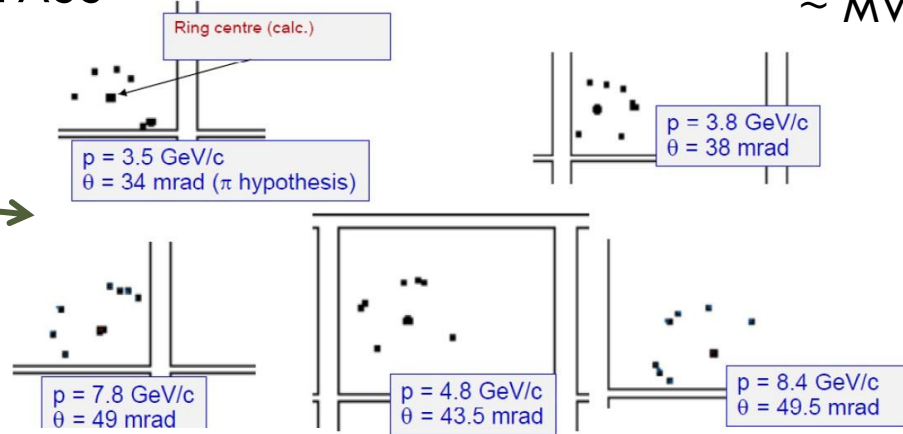
# PERFORMANCE

MPGD-based PDs used during COMPASS runs 2016, 2017, 2021, 2022

IBF: 3%

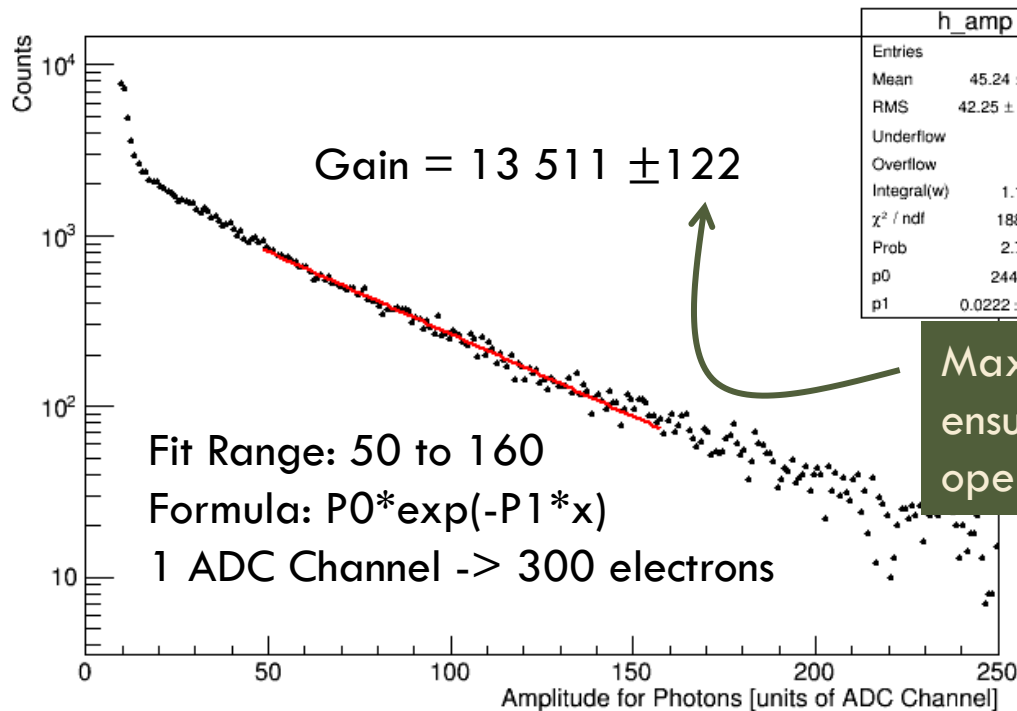
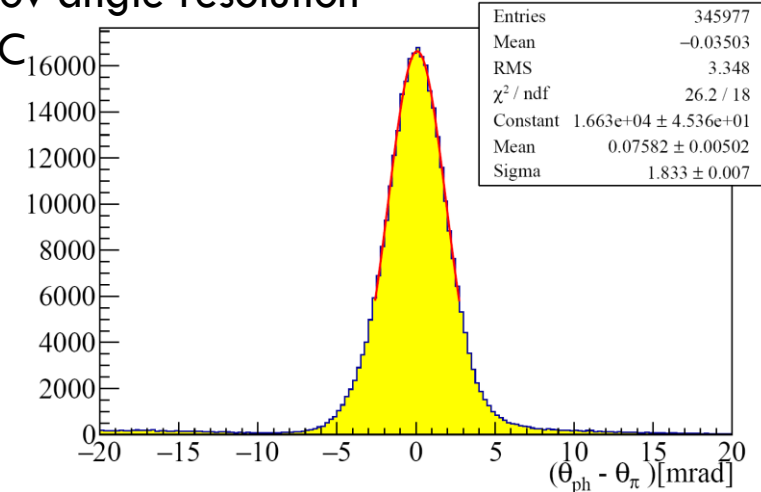
Electronic noise: 900ENC

Cherenkov rings in MPGD PDs  
- no background subtraction

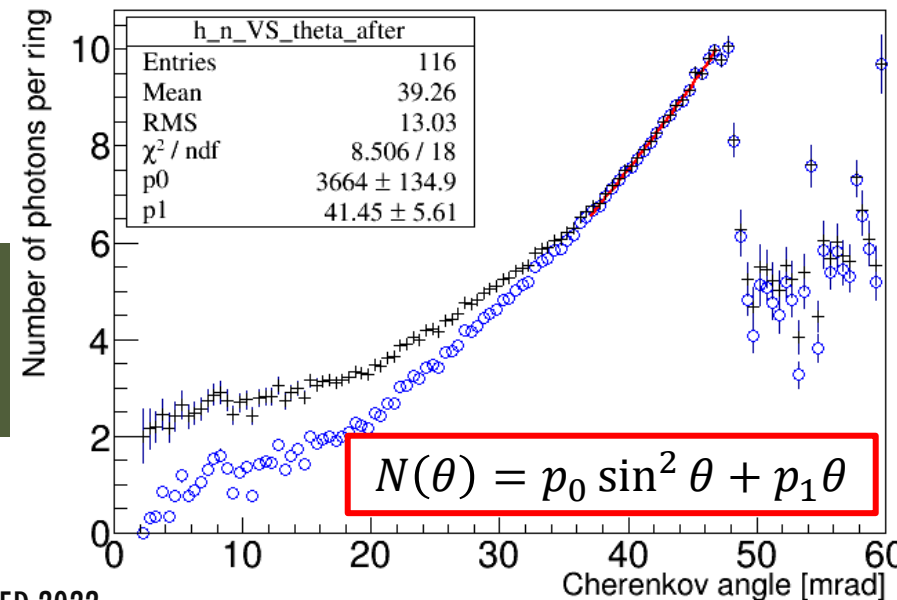


Cherenkov angle resolution

~ MWPC



Max gain that ensures stable operation

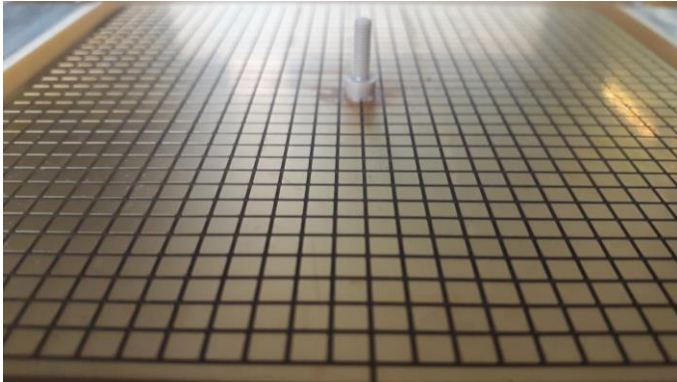


+ data points  
○ Poissonian correction

At saturation:  
11 photons

# A LOOK TO THE FUTURE

For exporting the technology to shorter radiator (e.g. collider experiment) >  
Improve space resolution

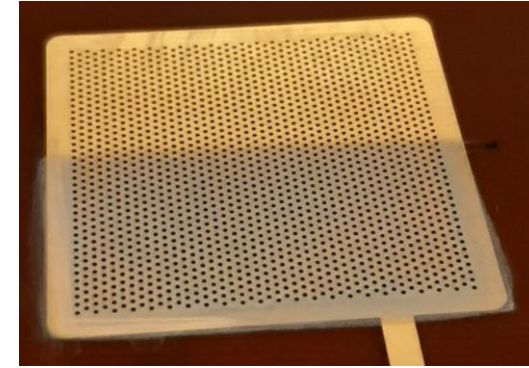


Reduced readout pad size ( $3 \times 3 \text{ mm}^2$ )

A prototype was produced and tested,  
promising results

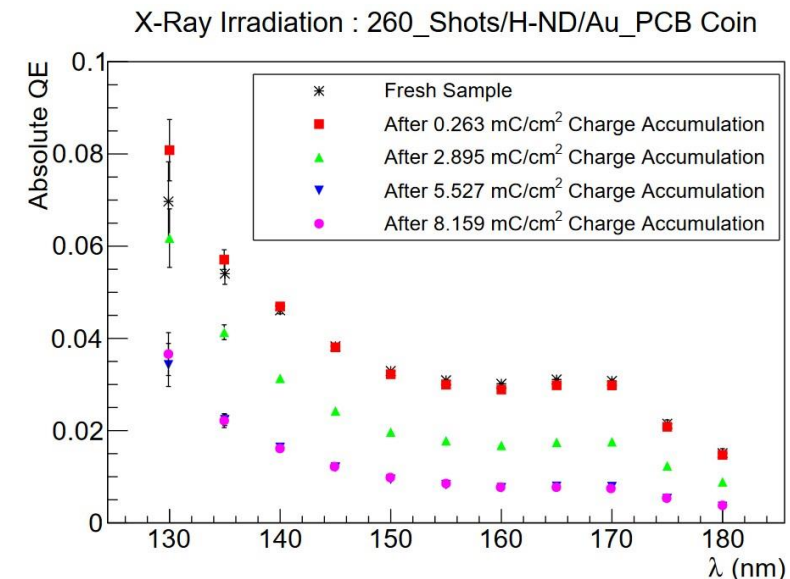
> non uniformity among pads requires  
careful design of anode plane

How low can we go in pad size?

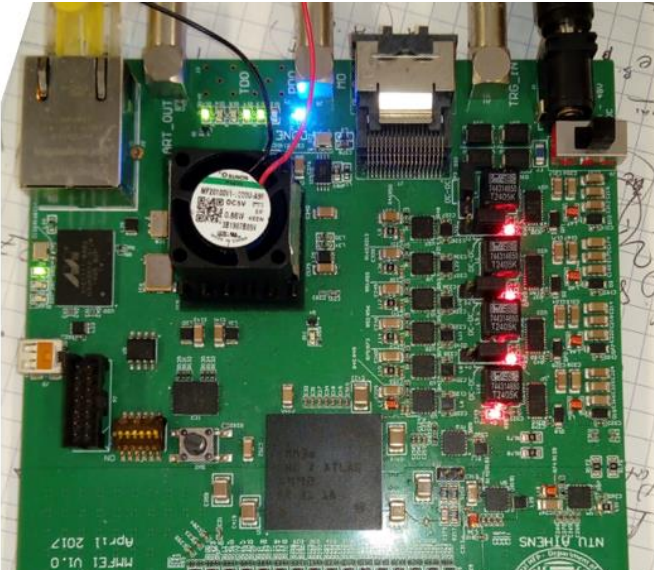


Novel photocathode: hydrogenated nanodiamond powder

- > Robust to ion bombardment
- > Easier to handle compared to CsI
- > QE comparable with CsI



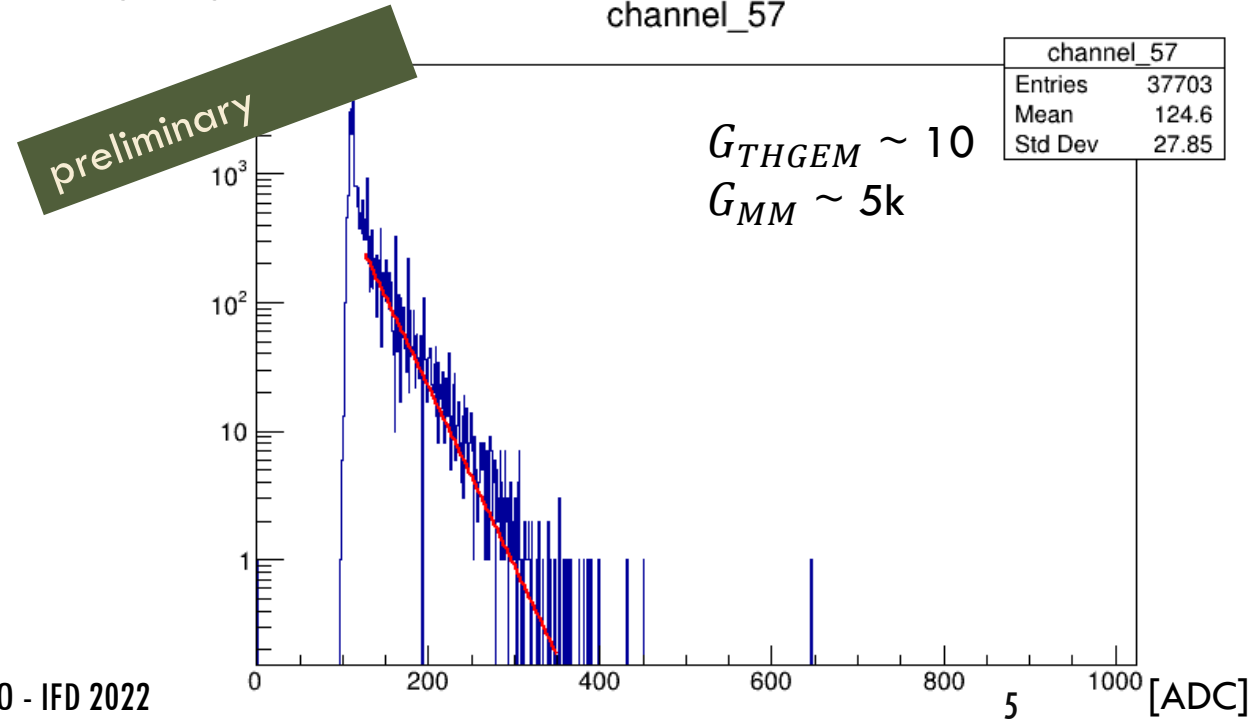
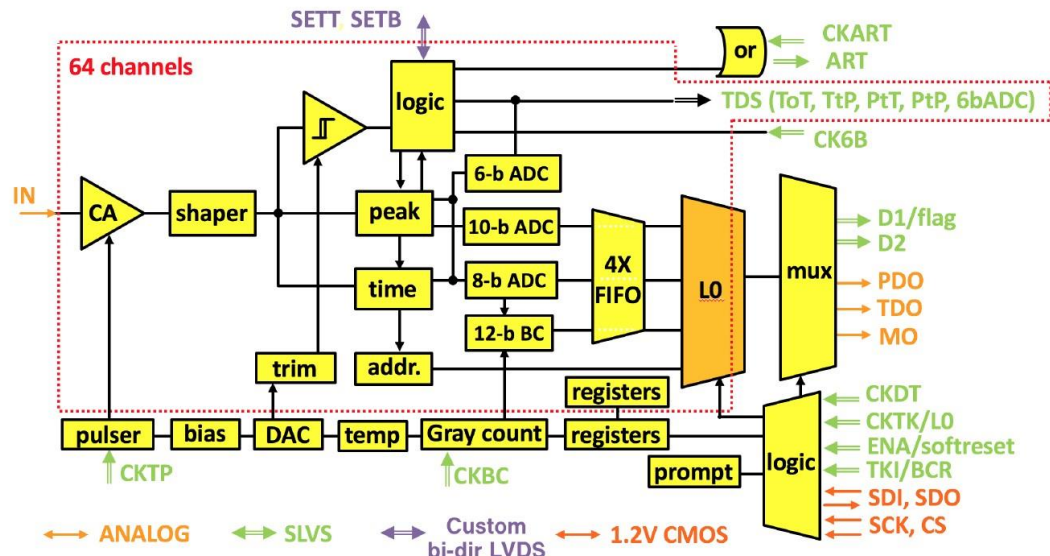
# A LOOK TO THE FUTURE



Single photon detection requires extremely low noise electronics

New Front-end electronics: VMM3a, designed for ATLAS NSW (MM and sTGC)

- > Compatible with triggerless DAQ
- > Each channel: CSA, Shaper, Discriminator, Digitizer
- > Output fully digital (time stamp, amplitude, n of channel, ...)
- > First tests with UV photons ongoing in Trieste



IFD 2022 : INFN Workshop on Future Detectors  
17-19 October 2022 Bari- Italy



IFD2022 - INFN Workshop on Future Detectors



Istituto Nazionale di Fisica Nucleare

- TWO SHOTS ON  
1. THE NEW NEUTRON HODOSCOPE  
2. RIBs CHARACTERIZATION FOR FRAISE, THE NEW  
FRAGMENT IN-FLIGHT SEPARATOR AT INFN- LNS***

***PAGANO EMANUELE VINCENZO (LNS-INFN)\* E  
MARTORANA NUNZIA SIMONA (LNS-INFN & UNICT)  
COLLABORAZIONE CHIRONE***

\* speaker



**FRAISE: a new FRAGMENT In-flight SEparator**  
**Approved inside POTLNS PON**

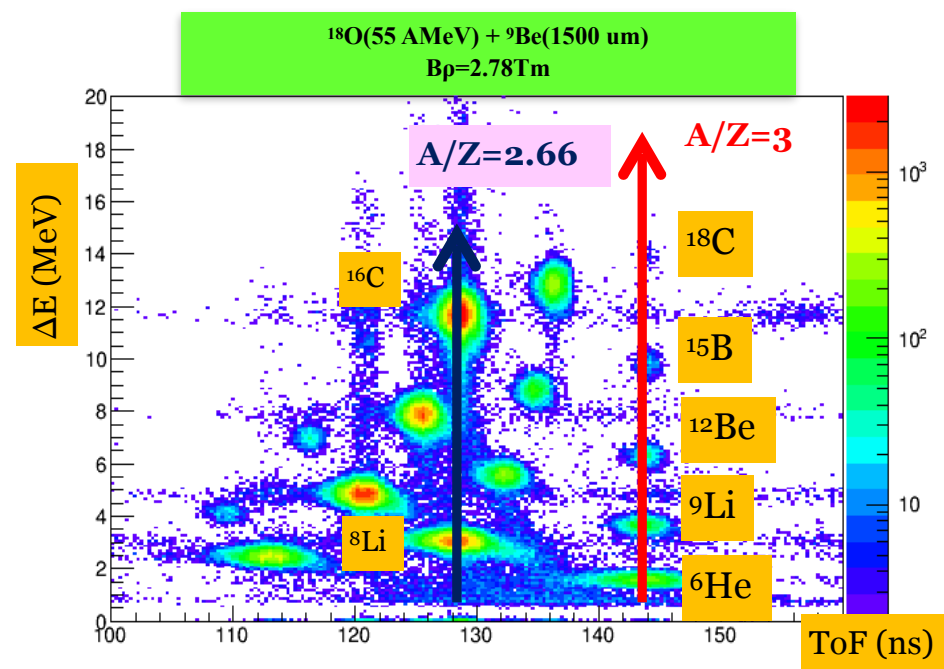
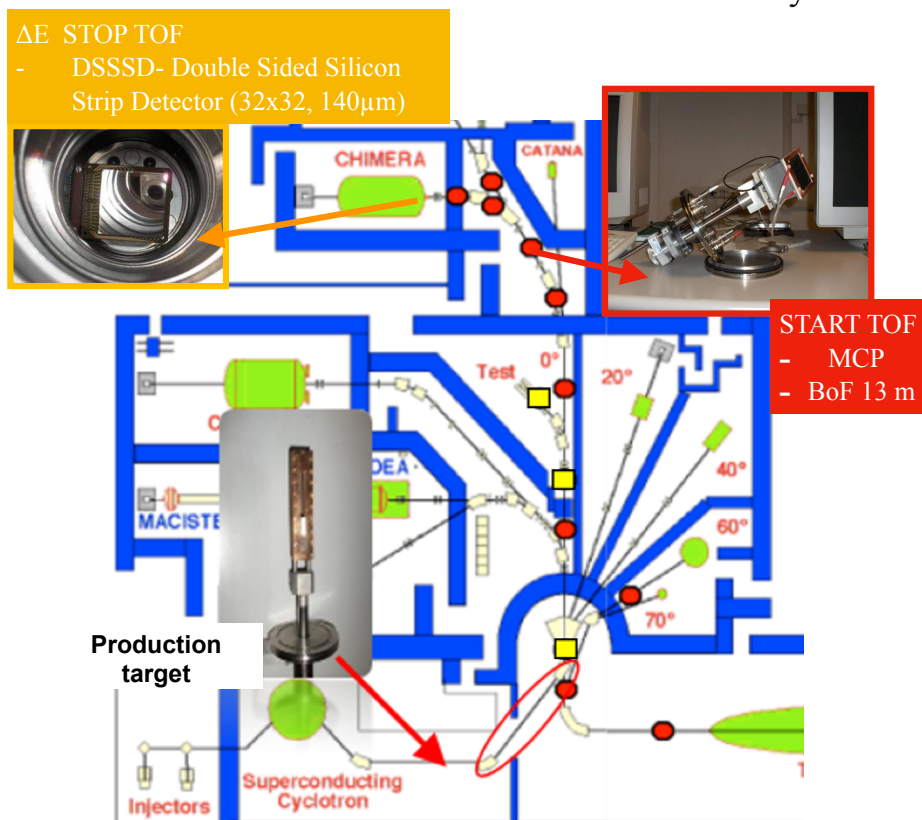
# What we did @FRIBs facility

At INFN-LNS RIBs were produced, from 2001 to 2019, using the FRIBs (in Flight Radioactive Ion Beams at LNS) facility through the In-Flight fragmentation employing a maximum beam power of 100 W

As known the produced beam is a «cocktail beam», we need :

- Diagnostics system DSSSDs + plastic scintillators, to achieve an optimal transport from the production target to the final user point
- Tagging device for the CHIMERA array ( $\Delta E$ -ToF method for PID identification, MCP-DSSSD system)

RIBs produced: from  ${}^6\text{He}$  to  ${}^{68}\text{Ni}$   
with max intensity of  $\approx 10^5$  pps



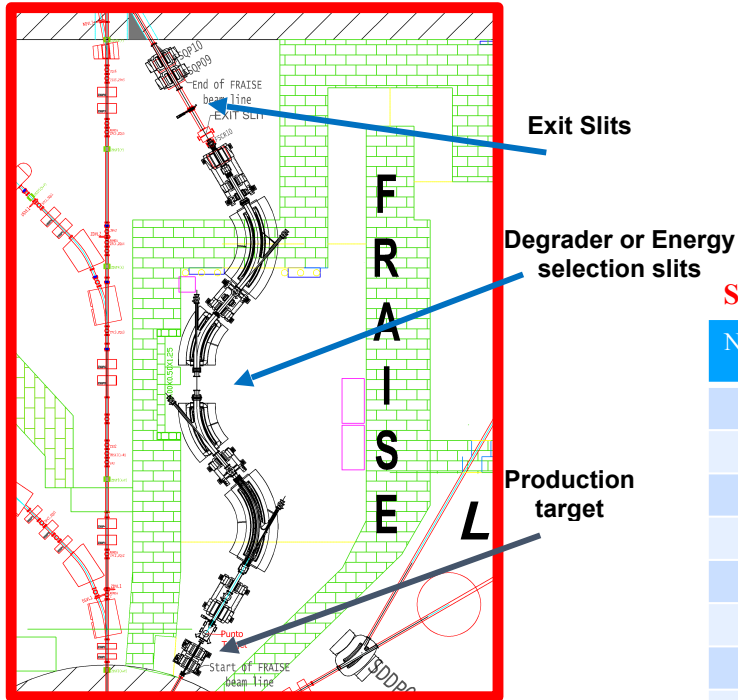
Characteristics:  
MCP: up to  $10^5$  pps,  $\Delta t \approx 200\text{-}300$  ps;  
DSSSD: max rate 200 kHz (light ions), 30 kHz (medium and heavy ions).  
Worsening of performances in  $\approx 1$  week;  
Time resolution  $\Delta t \ll 1$  ns ;

Lombardo I. et al., Nucl. Phys. B Proc. Suppl., 215 (2011) 272

# FRAISE: a new FRAGMENT In-flight SEparator

## Approved inside POTLNS PON

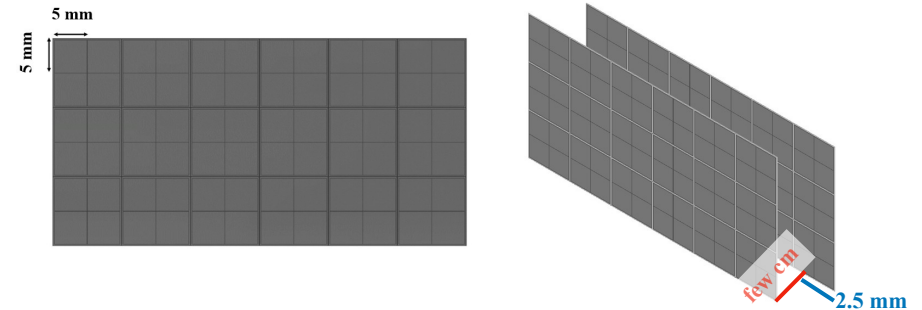
The building of a new fragment separator FRAISE (Fragment In- Flight Separator) is ongoing at INFN-LNS to provide high intensity ( $10^3 - 10^7$  pps) RIBs using the In-Flight Fragmentation method and employing a primary beam power of 2-3 kW. We expect an increasing up to two order of magnitude to the respect of the preset situation.



Some examples ( $E/A \approx 50$  MeV)

Nuclide of interest	Intensity* (kHz)
$^8\text{B}$	3100
$^{14}\text{Be}$	3
$^{13}\text{N}$	23000
$^{14}\text{O}$	1400
$^{16}\text{C}$	14000
$^{17}\text{F}$	170000
$^{19}\text{O}$	2300
$^{34}\text{Ar}$	8200

100  $\mu\text{m}$  thick fully depleted SiC rad-hard multi-pad sensors: up to  $10^7$  pps over the whole system with  $\Delta t \approx 200$  ps ( $\approx 0.1\%$  precision on energy for 20 m base-of-flight) if 200  $\mu\text{m}$  inter-pad dead zone, 10% dead area



- Front-end: Custom multi/channel ASIC with charge preamplifier configuration and analog pre-processing optimized for amplitude and time measurements
- Full waveform digitizers and synchronization with CHIMERA/FARCOS DAQ

New radiation-hard tagging systems are needed to measure features of RIBs:

- Need of a point-to-point measurement of cocktail intensity, relative composition (PID), energy distribution, 2D profile, angular distribution during optimization
- Monitoring of beam properties, start time for event-by-event ToF/energy measurement during data taking

Martorana N.S., Il Nuovo Cimento 44 C (2021) 1  
 Martorana N.S. et al., Il Nuovo Cimento 45 C (2022) 63  
 Russo A.D. et al., Nucl. Instrum. Methods B, 463 (2020) 418  
 Russotto P. et al., J. Physics: Conf. Ser., 1014 (2018) 012016  
 F. Risitano, Tesi di Laurea Magistrale, Università degli Studi di Messina, Italy

# NArCoS (Neutron Array for Correlation Studies)

## Idea for a new Neutron Hodoscope

**To realize a prototype of detector able to detect at the same time charged particles and neutrons with high energy and angular resolution for reaction studies and applications**

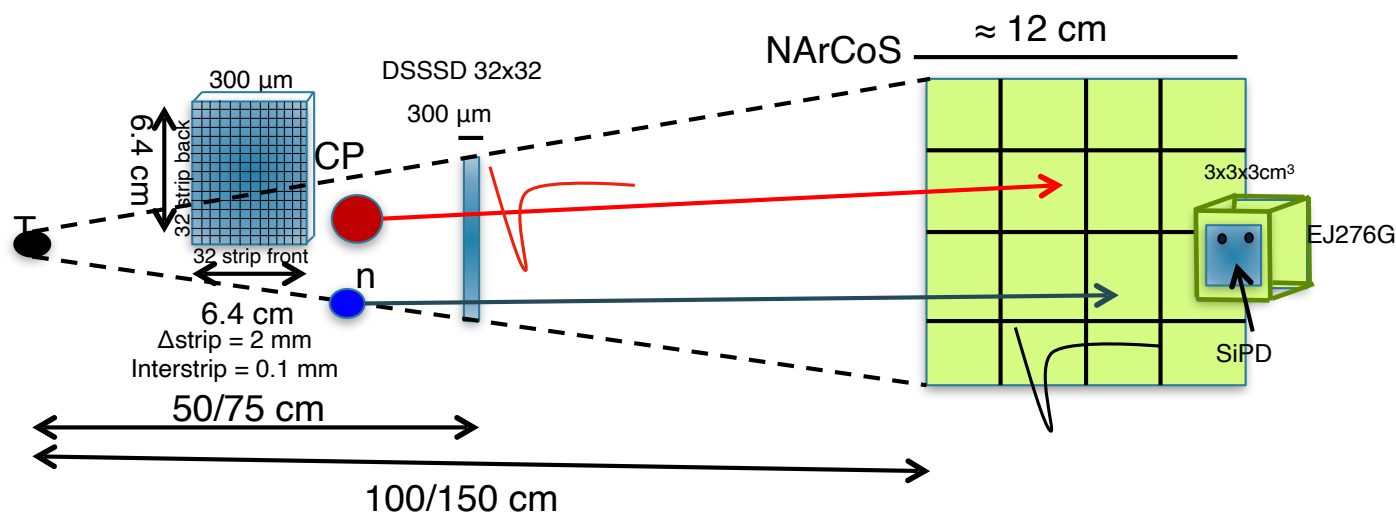
### Detector

- Candidate: The plastic scintillator EJ276-Green Type (ex EJ299-33) (3x3x3cm<sup>3</sup>)
- 1 cluster: 4 consecutively cubes -> 3x3x12 cm<sup>3</sup>
- Neutron detection efficiency  $\approx 50\%$  for the prototype
- Reading the light signal: Si-PM and digitalization
- Modular, reconfigurable (in mechanic and electronic)
- Discrimination of n/ $\gamma$  from PSD (but also light charged particles)
- Energy measurement from ToF ( $\Delta t \leq 0.5$  ns with  $L_{\text{ToF}} \approx 1 \div 1.5$  m)

TOF measured using the RF of the CS or with an ancillary MCP (low intensity exotic beams)

### Physic cases

- Neutron-particles correlations (HBT)
- Reaction Dynamics and time scale
- Symmetry Energy in EoS of nuclear matter
- Nuclear structure of unbound exotic nuclei
- In medium nuclear interaction
- Nuclear astrophysics (neutron stars and nucleosynthesis processes)
- Medical application (neutron production cross section, differential cross sections)





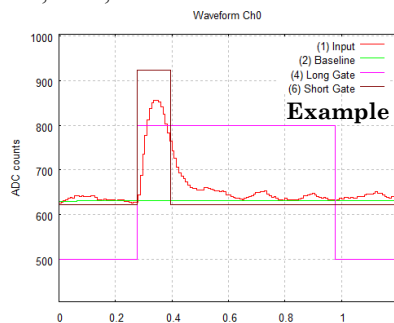
# PSD studies using sources

## > Detector Configurations:

- > EJ-276G + PMT
- > EJ-276 + i-Spector
- > EJ-276G + i-Spector

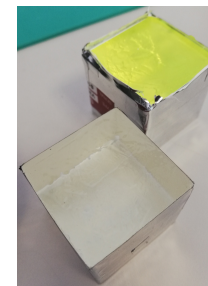
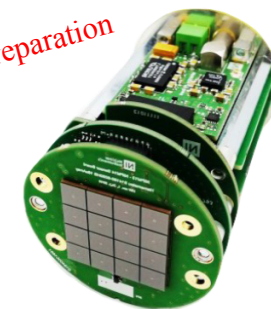
## > Lab measurements with radioactive sources:

- > Vacuum Chamber
- > Pb shield
- > Gamma sources:  $^{133}\text{Ba}$ ,  $^{137}\text{Cs}$ ,  $^{60}\text{Co}$ ,  $^{152}\text{Eu}$
- > Alpha source:  $^{241}\text{Am}$
- > Digitizer from CAEN



Example of signal and integration windows

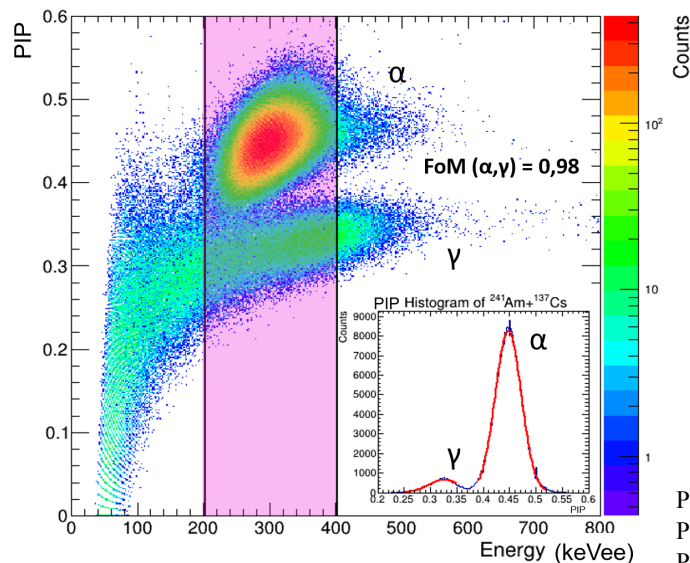
E.V.Pagano, G. Politi, A. Simancas et al., in preparation



Particle Identification Parameter

$$PIP = 1 - \frac{Q_{fast}}{Q_{tot}} = \frac{Q_{slow}}{Q_{tot}}$$

PIP vs. Energy of  $^{241}\text{Am} + ^{137}\text{Cs}$  002



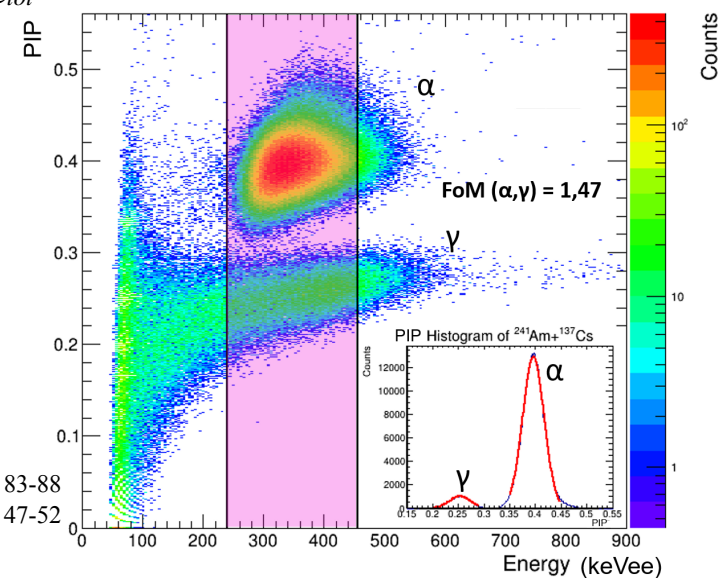
EJ-276 + i-Spector

## Results

Detector	FoM
i-Spector + EJ-276	0.98
i-Spector + EJ-276G	1.47
PMT + EJ-276G	1.03

- Pagano E.V. et al., N.S., Nucl. Instrum. Methods A, 889 (2018) 83-88
- Pagano E.V. et al., N.S., Nucl. Instrum. Methods A, 905 (2018) 47-52
- Pagano E.V. et al., IL NUOVO CIMENTO 41 C (2018) 181
- Pagano E.V. et al., JPS Conf. Proc. 32, 010096 (2020)
- Pagano E.V. et al., IL NUOVO CIMENTO 43 C (2020) 12
- Pagano E.V. et al., J. Phys.: Conf. Ser. 1643 (2020) 012037
- Pagano E.V. et al., IL NUOVO CIMENTO 45 C (2022) 64

PIP vs. Energy of  $^{241}\text{Am} + ^{137}\text{Cs}$  001



EJ-276G + i-Spector

# The LHCb RICH Upgrade

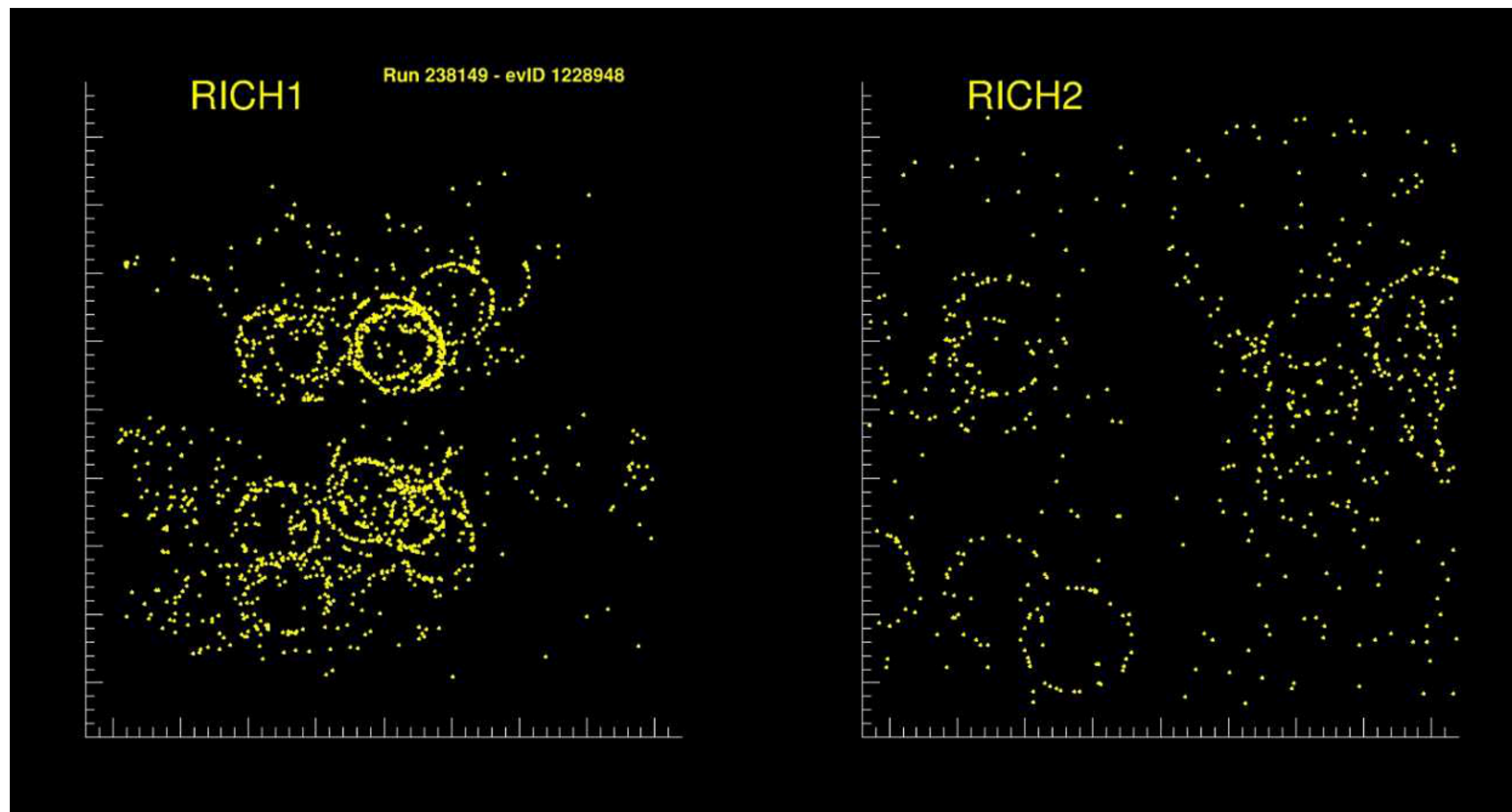
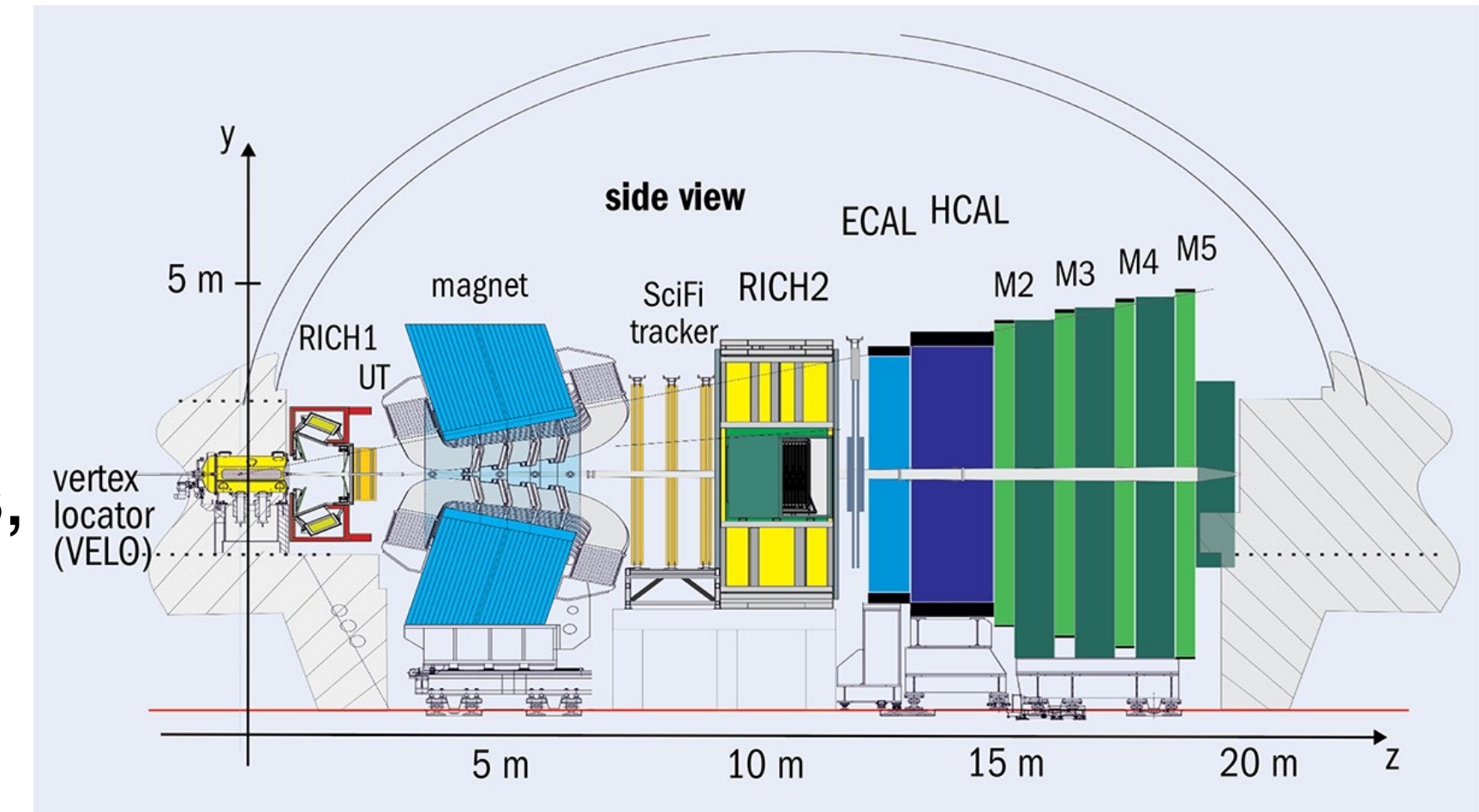
Federica Borgato on behalf of the Italian RICH groups  
*INFN Workshop on Future Detectors, 18th October 2022*



# The LHCb RICH detectors

LHCb relies on the **Ring Imaging Cherenkov (RICH) detector** system for the charged hadron identification in the momentum range [2;100] GeV/c.

The **Cherenkov light** produced by those particles is redirected by an **optical system** towards the **photodetector planes**, composed by **Multi-Anode PMTs**, and outside the acceptance of the spectrometer.



The **commissioning** of the current **RICH detector** (Upgrade 1a) is ongoing.

Upgrade 1a	Long Shutdown 2
Upgrade 1b	Long Shutdown 3
Upgrade 2	Long Shutdown 4

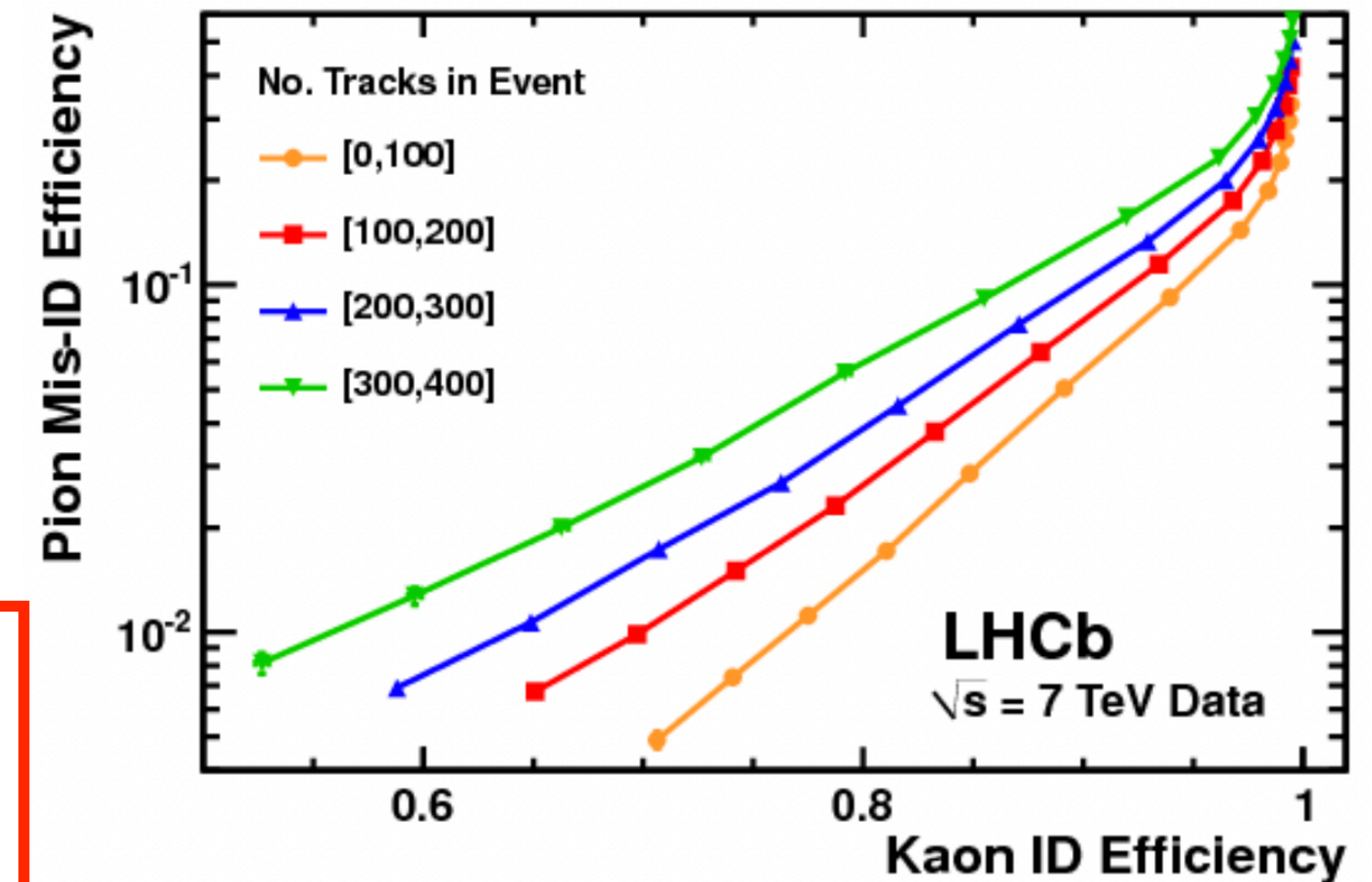
# The LHCb RICH in Upgrade 1b/2

The **PID** performance is affected by **high detector occupancy**

→ In **Upgrade 1a** the expected maximum occupancy is  $\approx 30\%$  and very non-uniform

## Upgrade 2 conditions:

- Keep or reduce maximum occupancy in the detector, make it more uniform, zooming into the high-occupancy central region
- Improve Cherenkov ring angle resolution



## Many requirements for Upgrade2!

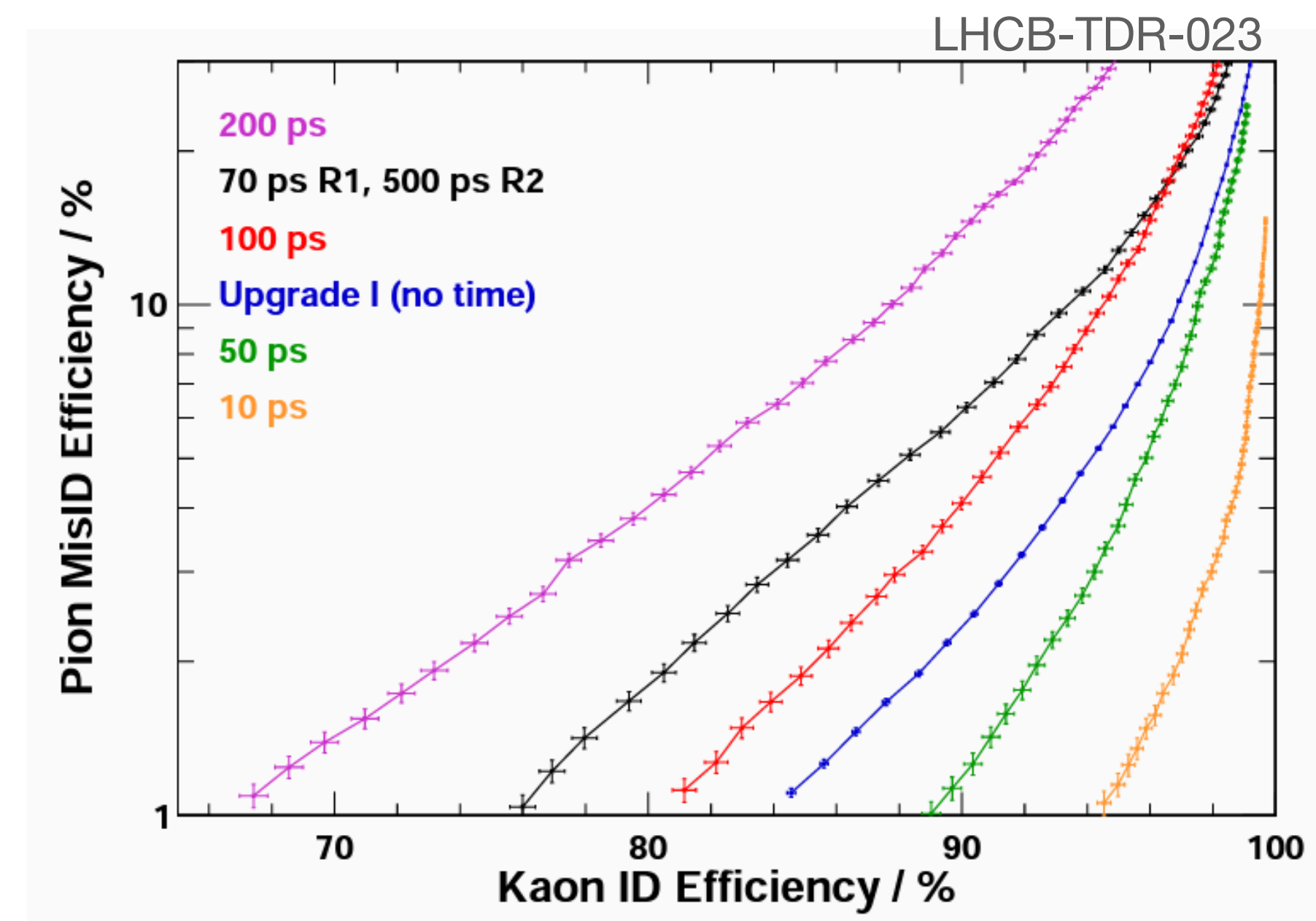
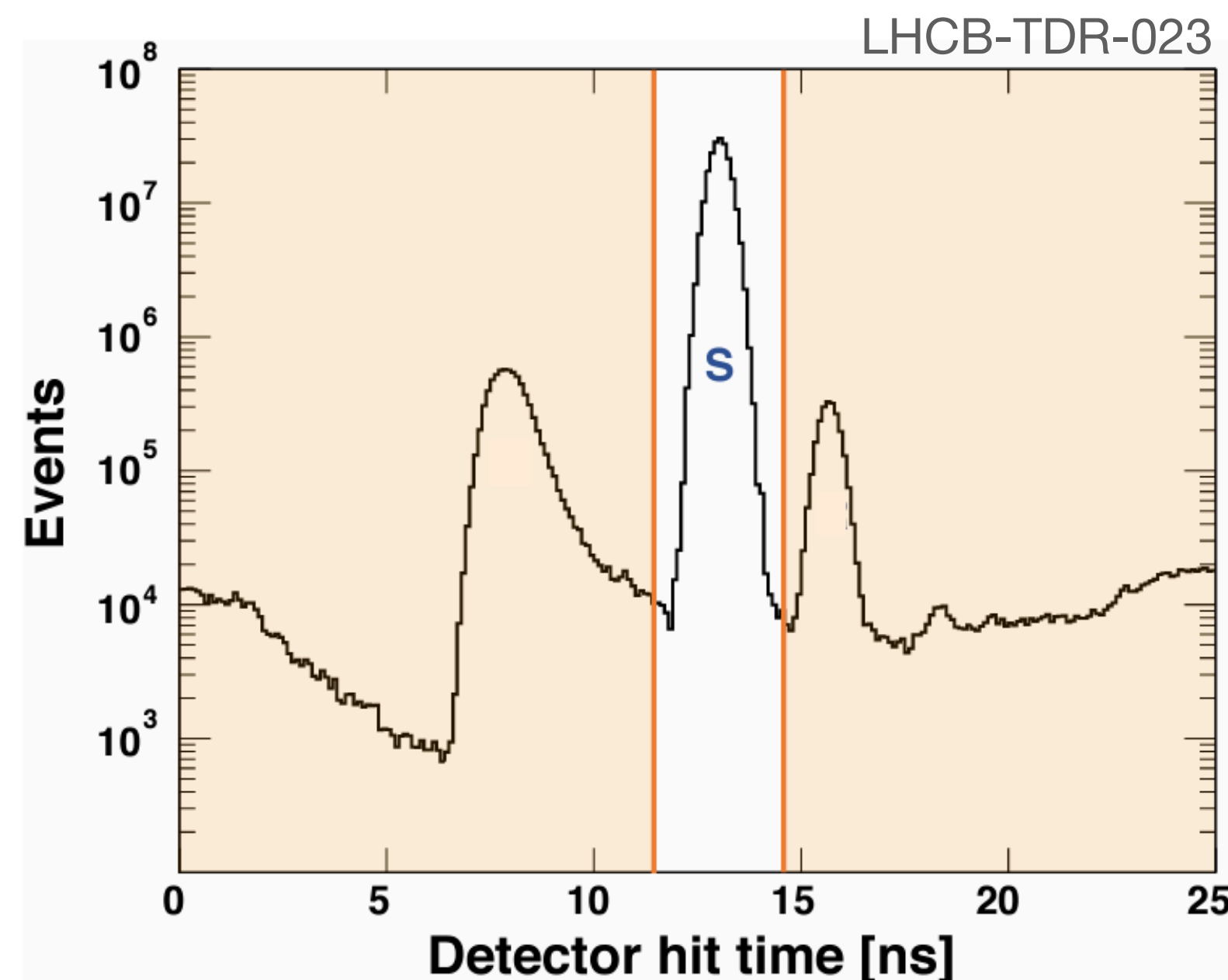
- Reduce occupancy → Reduce pixel size to focal length ratio, extend readout to include timing, change optical design
- Improve Yield → New photo-sensors with enhanced overall photo-detection efficiency
- Improve pixel size error → Reduce pixel size to focal length ratio
- Improve chromatic error → Improve  $\sigma_{chromatic} / \sqrt{N}$
- Improve emission error → New optical design

# RICH PID with timing in Upgrade 1b/2

**Cherenkov photons** from a given track arrive almost **simultaneously** (about tens of ps) and it is possible to **predict the time of arrival of photons** from a track with an **excellent precision**.

Using a **fast timing information** would allow to **improve the RICH PID performance**:

- **Nanosecond-scale time shutter** around the expected RICH detector hit time (Upgrade 1a-b)
- **10 picosecond-scale timestamp of photon hits** to be compared to the predicted time in the event reconstruction (Upgrade 2)



# Photodetectors for Upgrade 1b/2

	SiPM	MCP-PMT	MaPMT
Time resolution [ps]	100	20	200
Pixel size	<1mm	<1mm	≈3mm
Bias voltage [V]	10-70	≈ 10 <sup>3</sup>	≈ 10 <sup>3</sup>
Dark count rate	✗	✓	✓
Radiation Hardness	✗	✓	✓
Gain Aging	✓	✗	≈



### SiPM

**PROs**

- High photon detection efficiency
- Good single photon time resolution
- Able to sustain high photon rates
- High granularity

**CONs**

- Radiation hardness
- High noise (dark count rates)

*R&D ongoing to improve those aspects!*

### MCP-PMT

Hybrid vacuum photo-detector development:  
Photocathode + MCP multiplication +  
Timepix4 anode in vacuum tube

**PROs**

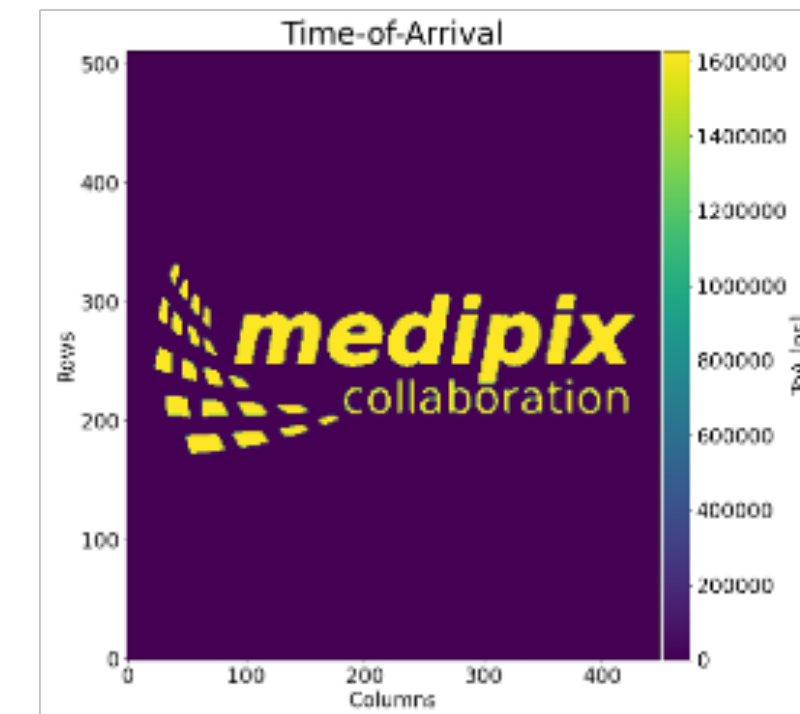
- Simultaneous excellent time and space resolution
- Low noise at room temperature
- Large active area

**CONs**

- High bias voltage
- Current saturation at high rates
- Ageing

# Hybrid MCP development

- Hybrid vacuum photo-detector development
  - Photocathode + MCP multiplication + Timepix4 anode in vacuum tube
  - Funded by ERC: 4DPHOTON (INFN, CERN, UniFE)
- Timepix4 ASIC productions: v0 (Q1-2020), v1 (Q4-2020), v2 (Q4-2021)
  - v2 bare ASIC extensively tested; first tests with Si sensor in summer 2022
  - ASIC, read-out electronics, software and expertise available to the INFN community (MEDIPX4 project in CSN5)

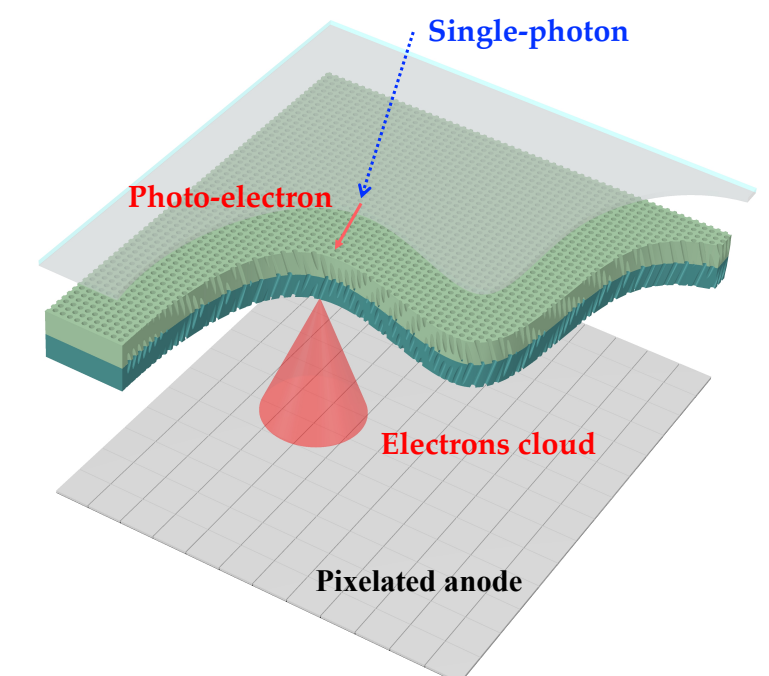


## Advantages:

- On-detector signal processing and digitization with large number of active channels (~230 k pixels), with limited number of external interconnections (~200)
- Longer lifetime due to low gain operation
- Excellent timing (<100 ps) and position (5-10  $\mu\text{m}$ ) resolutions
- Timing resolution and radiation hardness can be improved with next generation ASICs (e.g. [PicoPix project](#) at CERN for future VeloPix2 ASIC, 20-30 ps TDC LSB, or Timespot)

## Cons:

- Saturation at high rates and ageing for large integrated charge





*IFD 2022*

INFN Workshop on Future Detectors, 17 - 18 October 2022, Bari

# ***SiPM studies for the ALICE 3 Aerogel RICH detector***

A. R. Altamura<sup>a</sup>, D. Di Bari<sup>b</sup>, A. Di Mauro<sup>c</sup>, E. Nappi<sup>a</sup>, N. Nicassio<sup>b</sup>, G. Volpe<sup>b</sup>

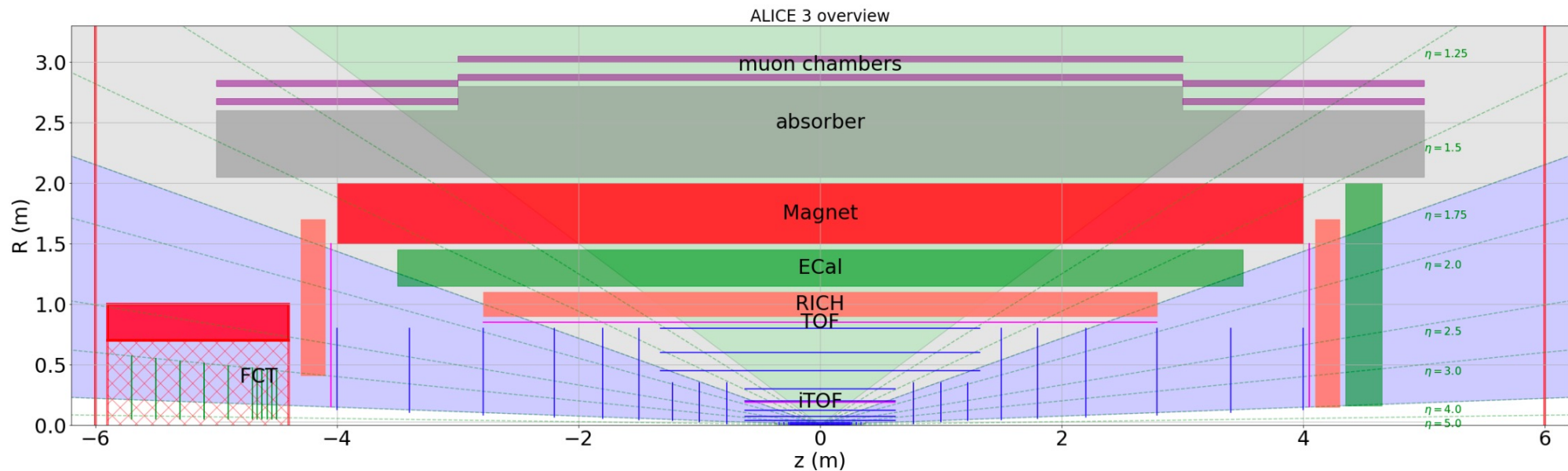
<sup>a</sup>*INFN, Bari, Italy*

<sup>b</sup>*University and INFN, Bari, Italy*

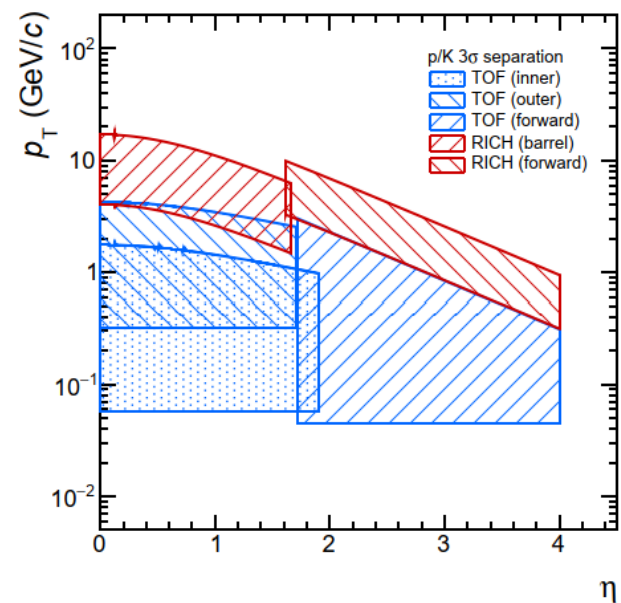
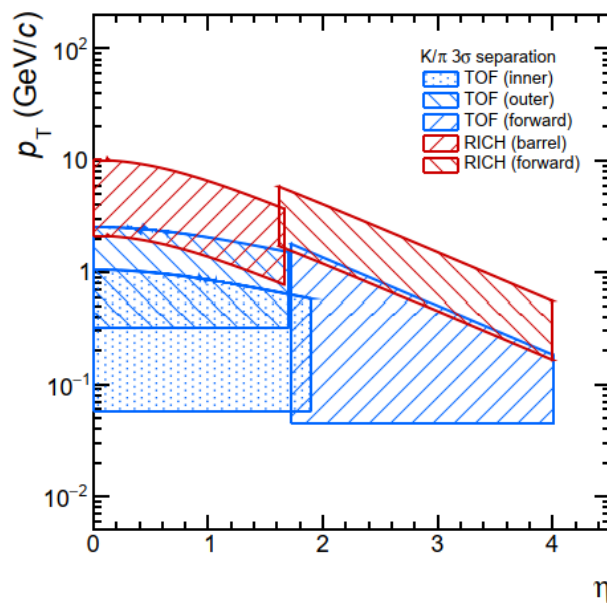
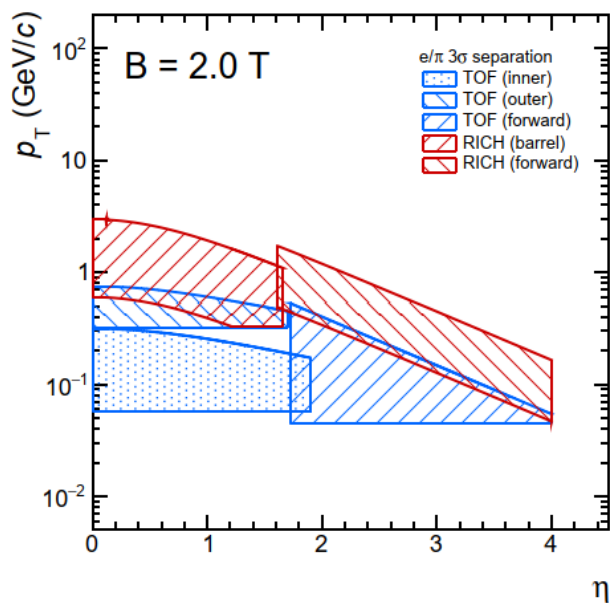
<sup>b</sup>*CERN, Geneva, Switzerland*



# RICH system in the ALICE 3 layout



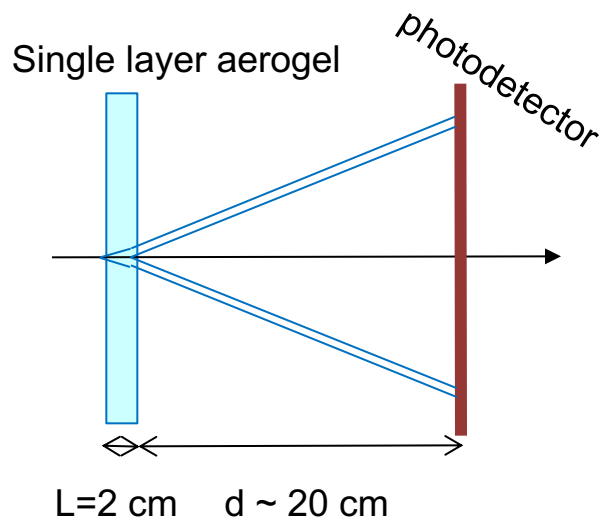
Extend electron and charged hadron ID at momenta higher than the TOF range



# Layout options and photon detector

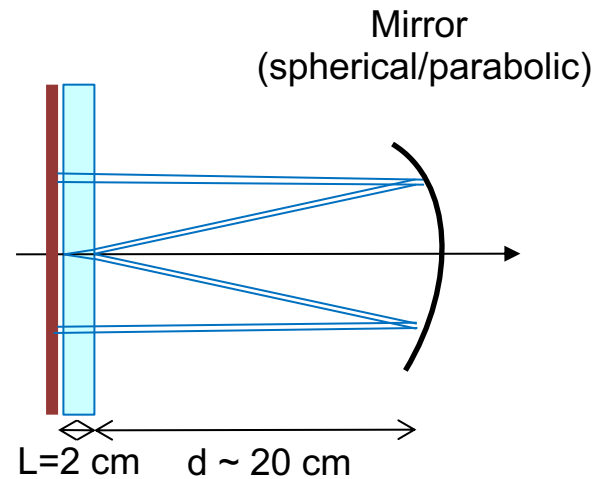
## Baseline layout:

- No aerogel focusing
- Aerogel layer @ 0.9 m from IP
- Photodetector @ 1.1 m
- Aerogel  $\sim 32 \text{ m}^2$ , p.d.  $\sim 39 \text{ m}^2$



## Mirror layout:

- With or w/o aerogel focusing
- aerogel layers @ 0.95 m from IP
- photodetector @ 0.9 m
- Aerogel  $\sim 33 \text{ m}^2$ , p.d.  $\sim 32 \text{ m}^2$



## Photon detector main requirements

- Single photon sensitivity in the visible range (Photon Detection Efficiency (PDE)  $> 40\text{-}50\%$ )
- Integration fill factor  $> 90\%$
- Pixel  $\sim 3 \times 3 \text{ mm}^2$
- Time resolution  $\sigma < \sim 100 \text{ ps}$
- Magnetic field  $B \leq 2 \text{ T}$
- Expected radiation load: NIEL  $\sim 10^{12} \text{ 1-MeV } n_{\text{eq}} / \text{cm}^2$

### → pro's:

- **Reduce/suppress geometric aberration** depending on mirror:
  - flat: doubling of gap
  - cylindrical: focusing in one direction + doubling of gap
  - parabolic: full focusing
- **reduce p.d. area by 60%**

### → con's:

- $\sim 20\%$  photon loss due to double crossing of aerogel and mirror reflection
- spherical aberration and mirror alignment to be taken into account

# The photon detector

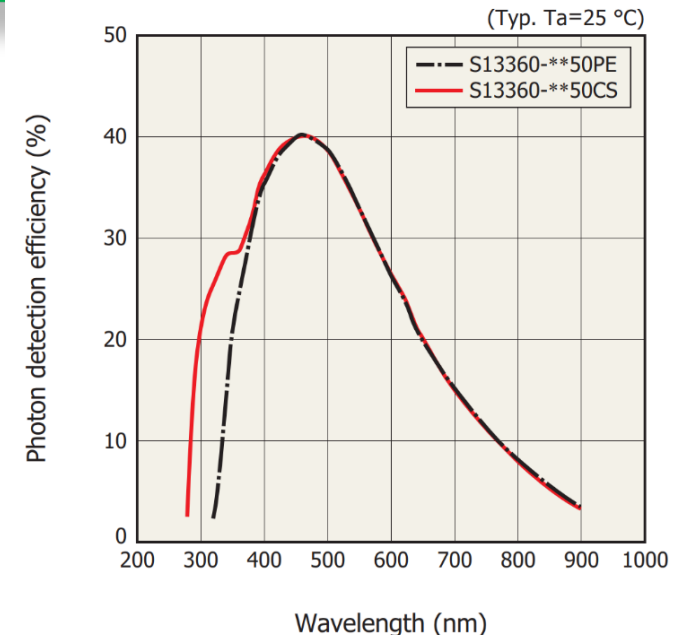
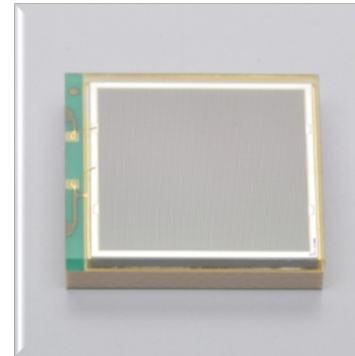
Significant enhancement on the semiconductor process over past decades, excellent improvement of CMOS SPAD performance → renewed interest for the **development of digital-SiPM** for large area coverage in HEP applications (e.g.: development ongoing in Sherbrooke University and FBK)

- **R&D on digital SiPM based on CMOS Imaging technology**

- Reduce cost
- Explore solutions for:
  - noise performance improvement (beyond online/offline time gate)
  - radiation hardness improvement (1-2 orders of magnitude,  $10^{12}$  1-MeV  $n_{eq}/cm^2$  required)
  - TOF applications (MIPs detection with time resolution  $\sim 20$  ps)

- **Backup option: commercial SiPM**

- Example: SiPM HPK 13360 3050CS
  - $3 \times 3$  mm<sup>2</sup> pixel (3600 SPADs with 50  $\mu$ m pitch)
  - Dark count rate (DCR)  $\sim 50$  kHz/mm<sup>2</sup>
  - 50 ps time resolution
  - Above  $10^{11}$  1-MeV  $n_{eq}/cm^2$  → DCR increasing



# A step forward: Cherenkov-based TOF system

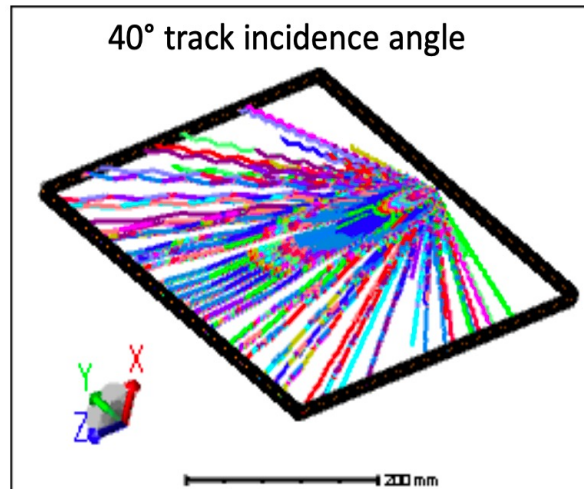
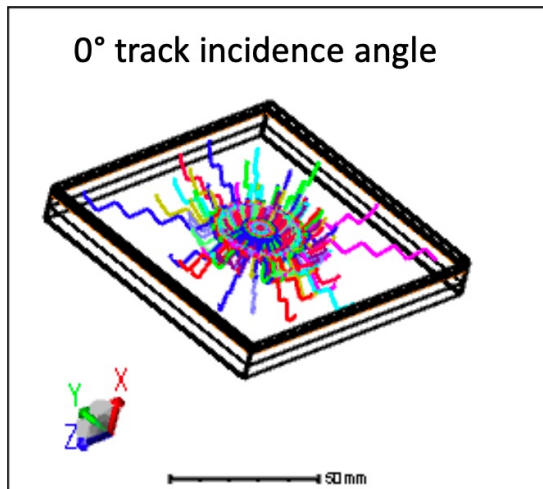
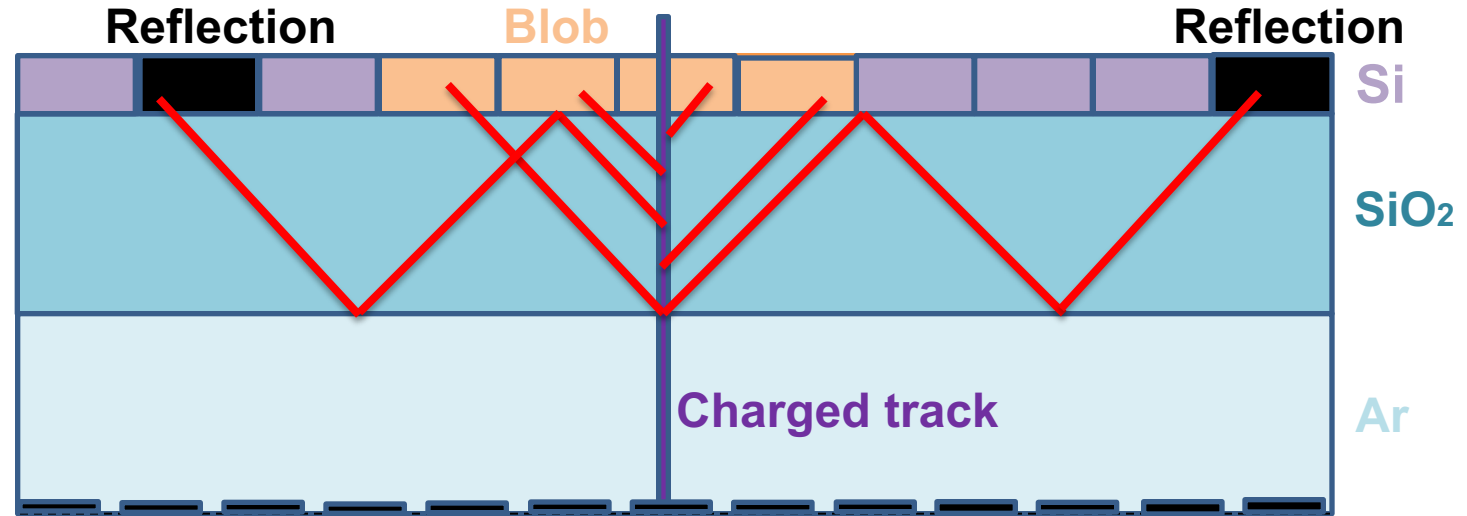
## Reflection background

About 30% of photons reflected at  $SiO_2 - Si$   
 Total reflection at  $SiO_2 - Ar$

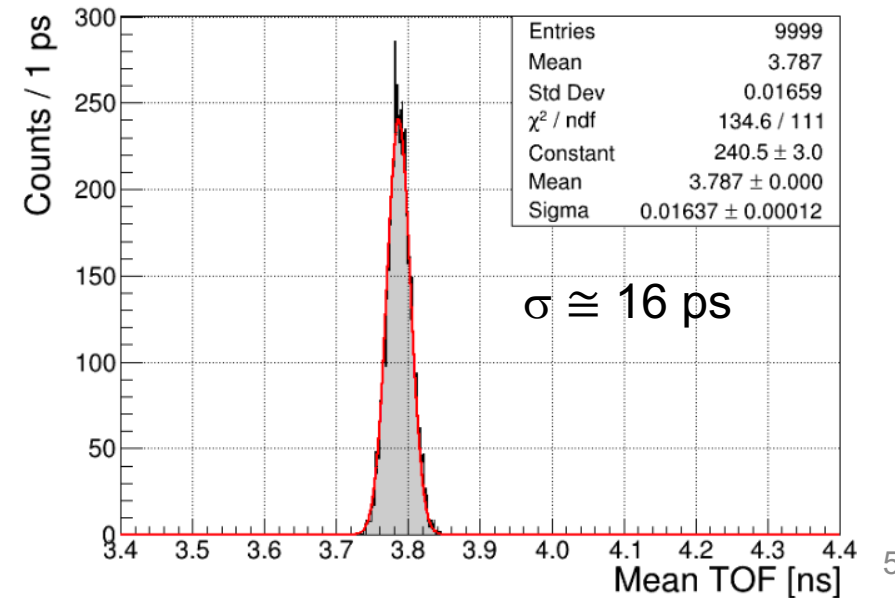
## Track time resolution

Determined by single photon resolution and  
 blob size

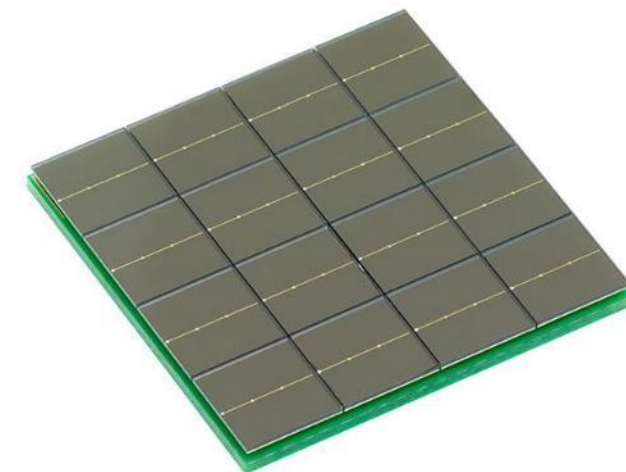
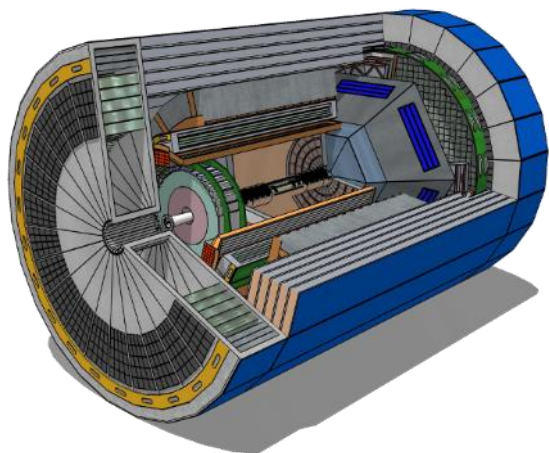
$$\sigma_{\theta_t}^{trk} = \frac{\sigma_t^y}{\sqrt{N_{blob}}}$$



1 mm Crown Glass, 3 mm<sup>2</sup> cells



# A SiPM-based optical readout system for the EIC dual-radiator RICH



**R&D on SiPM as potential photodetector for dRich**

# The EIC

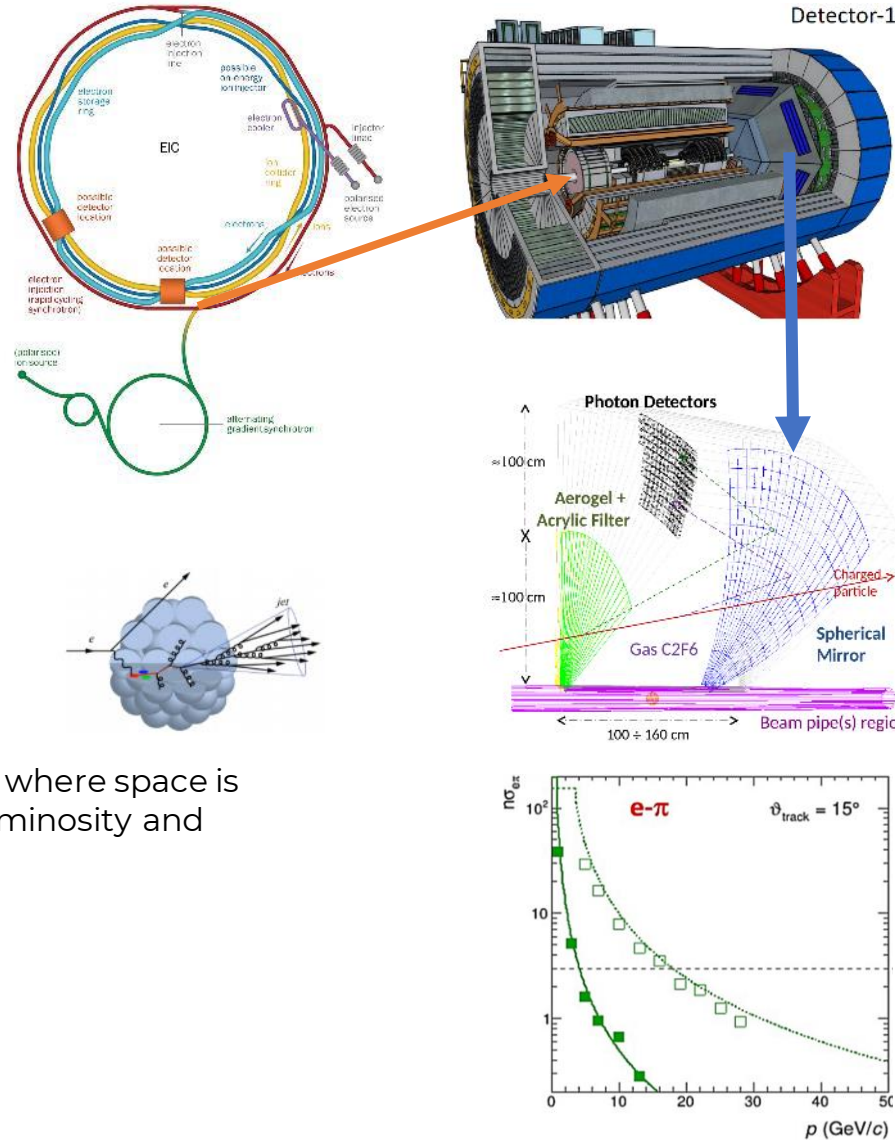
The **Electron Ion Collider (EIC)** will be a large-scale innovative **particle accelerator** planned to be built at **Brookhaven National Laboratories** in Long Island, New York (U.S.A.). Constitutes the **major project** in the **nuclear physics** field.

Highly **polarized electrons** collide with **protons** and **nuclei** providing access to those regions in the nucleon and nuclei where their structure is dominated by gluons. **Polarized beams** in the **EIC** will give unprecedented access to the **spatial** and **spin structure** of the **proton, neutron, and light ions**

The **EIC** covers a **center-of-mass** energy range for **e+p** collisions of  $\sqrt{s}$  of **20 to 140 GeV**  
The **first beam** operations are expected to start in the **early 2030s**.

The EIC detectors are in the interaction regions where space is constrained due to the requirements of high luminosity and will have:

- Tracking and Vertexing Detector Systems
- **Particle Identification Detector Systems**
- Calorimeter Detector Systems



A dual-radiator (**dRICH**) is in charge for the forward **Particle Identification PID**. It is compact and cost-effective solution for continuous momentum coverage (3-60 GeV/c). It shows interesting capability in the electron-pion separation.

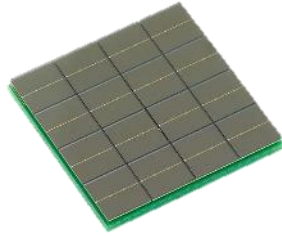
**Radiators** are made in aerogel ( $n \sim 1.02$ ) and C2F6 ( $n \sim 1.0008$ ).

**Mirrors:** large outward-reflecting, 6 open sectors.

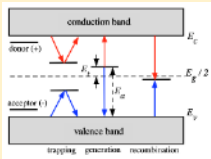
The Photon Detectors is made by  $3 \times 3 \text{ mm}^2$  **SiPMs** arranged in **six**  $0.5 \text{ m}^2$  / sector for a total of **3 m<sup>2</sup>** surface ( $\sim 300 \text{ k}$  channels). The SiPM technology allows **single-photon** detection inside high B field ( $\sim 1 \text{ T}$ ). SiPMs have **fast time resolution** but there are consideration on **dark noise** and **radiation hardness**.

SiPMs are a valuable option for the **dRICH** optical readout:

- Cheap
- Low voltage operation
- Excellent time resolution
- Single photon detection
- Insensitive to magnetic field
- High spatial resolution
- **High noise as Dark Count (DCR)**
- **Prone to radiation damage ( $10^{11} n_{eq}/cm^2$ )**

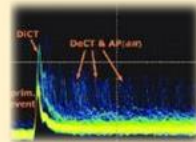


DCR is reduced by a factor 40 every 30° C of temperature reduction. The dRICH SiPMs will be operated at **-30° C**.



Radiation damage is produced by Non-ionizing Energy Loss (NIEL) leading to **displacement** damages and build up of **crystal defects** that results in:

- Increased **DCR**
- Increased **After Pulses**
- Change in **charge collection**



Performance can be recovered by using **annealing techniques**. High temperature re-order out-of-lattice atoms to their former positions reconvening performance

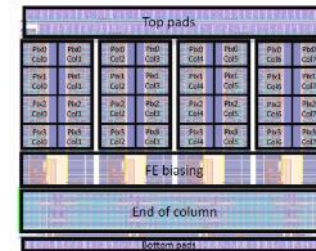
- <https://arxiv.org/pdf/1805.07154.pdf>,
- <https://www.osti.gov/pages/servlets/purl/1477958>,
- <https://ieeexplore.ieee.org/document/9059772>,
- <https://arxiv.org/abs/1804.09792>

**3x3 mm<sup>2</sup> SiPMs from different vendors and with different cell sizes are mounted in matrixes were studied to evaluate their performance after irradiation and annealing.**

Vendor	Version	Cell size (μm)	V <sub>BD</sub> (V)	DCR (kHz/mm <sup>2</sup> )
Hamamatsu	S13360-3050VS	50	53	55
Hamamatsu	S13360-3025VS	25	53	44
Hamamatsu	S14160-3050HS	50	38	160
Hamamatsu	S14160-3015PS	15	38	78
FBK	NUV-HD-CHK	40	31	50
FBK	NUV-HD-RH	15	31	40



FBK matrix



ALCOR scheme

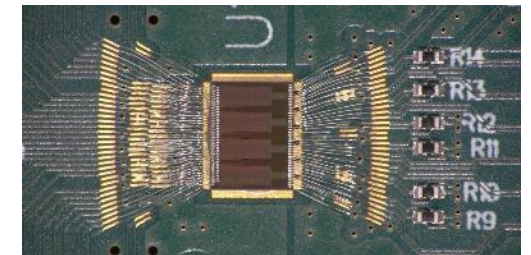


Hamamatsu matrix

The **ALCOR-ASIC** (developed by INFN-TO) is a **32-pixel** matrix mixed signal with a dual polarity **frontend** for **amplification** and **conditioning**.

Each pixel features

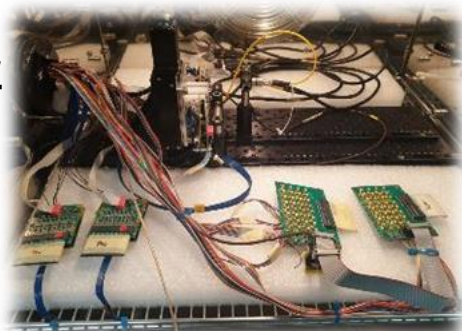
- dual-polarity front-end amplifier
- 2 leading-edge discriminators
- 4 TDCs based on analogue interpolation



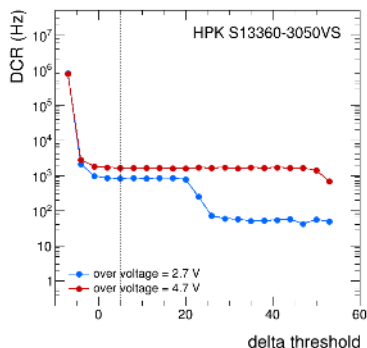
To mimic the **operative conditions**, sensors are tested in a **climatic chamber** at **-30° C**.

3 different automated measures are performed in parallel on the matrixes:

- Dark Count Rates (**DCR**)
- Current over Voltage curves (**IV**)
- Light response (**PDE**)



**Test set-up**



**DCR** is measured by the full dressed **ALCOR redout**. The ASIC streams **TDC** hits to an **FPGA** through a LVDS. **Threshold** and bias **voltage scan** are used to automatically compute the threshold level and the bias voltage.

**IV** curves are measured by a Keithley 2450 **SMU** and a **multiplexer** (up to **64 SiPMs**) to measure the **Dark Current**.

For the **PDE**, a sensor's matrix is mounted on a 2-axis stage. The fixed **LED** source ( $\lambda = 570$  nm) is powered with a pulser at **1 MHz** for **50 ns**. The number of **counts** measured in **coincidence** with the pulser is compared to the same measure of a **reference sensor** to evaluate **losses** in the **PDE** after the **irradiation/annealing**



Detectors are **characterized before** and **after the irradiation** at **TIFPA**.

Irradiation at **INFN TIFPA** facility in Trento with **148 MeV protons**.

Differential approach to test **different levels** of damage ( $10^8$ - $10^{11}$   $n_{eq}/cm^2$ ).

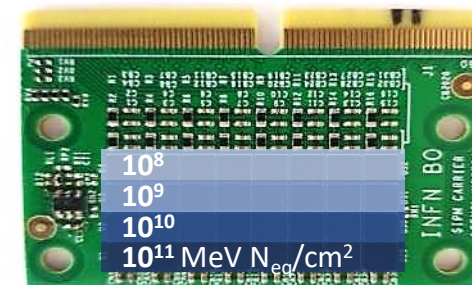
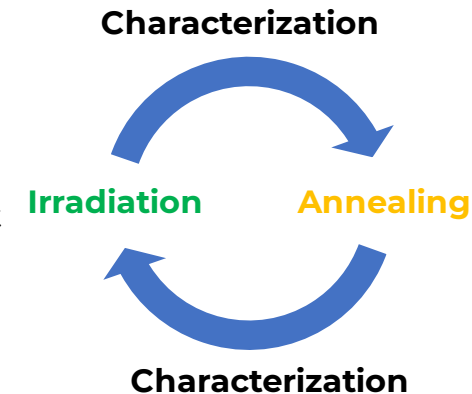
**After the annealing** they are **characterized** again.

The **annealing** is performed in a **temperature-controlled oven** at **150° C** for **200 hours** in Ferrara.

More than **150 SiPMs** undertook this **cycle**.

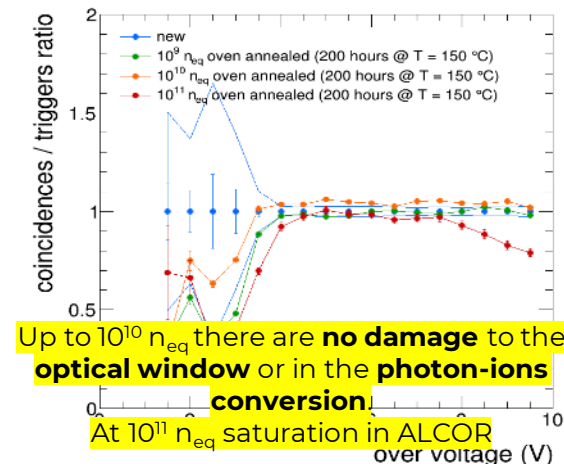
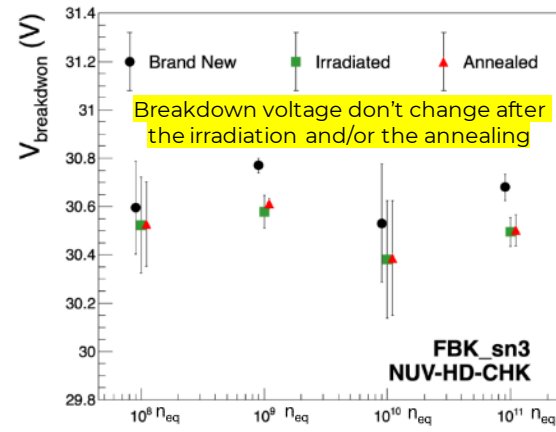
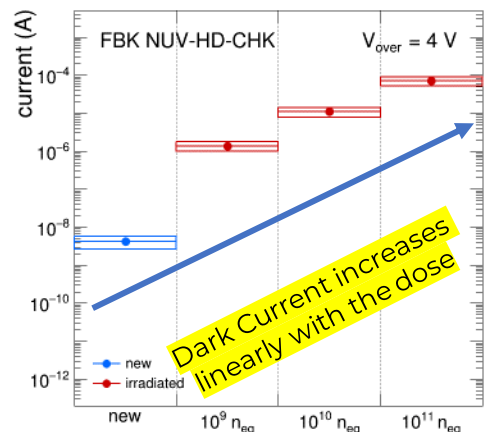
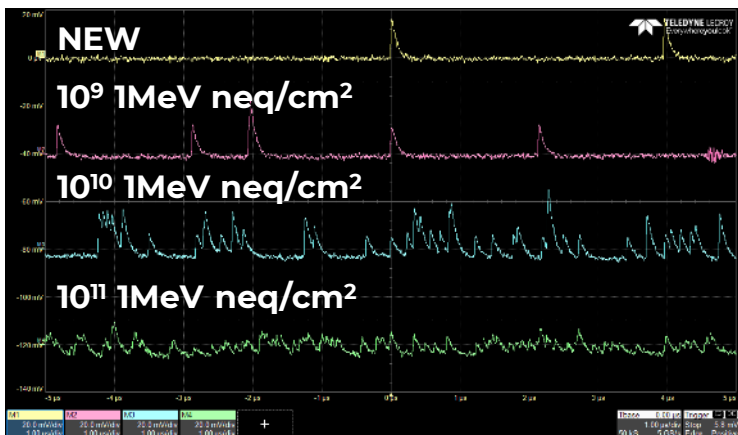
### Current annealing

If directly polarized, **current** flows into the **SiPM**, **heat** is generated and contributes to the **annealing**. For a small sample of devices, a new method of direct current annealing is tested @**175° C** for **2.5 hours**.

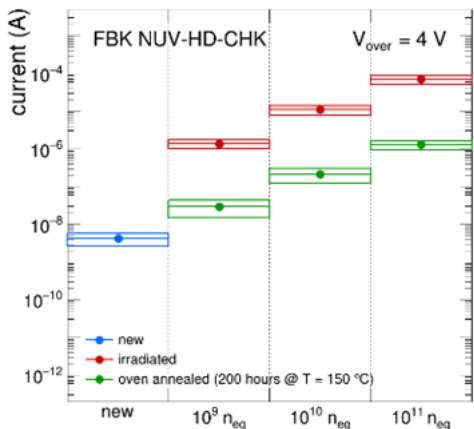




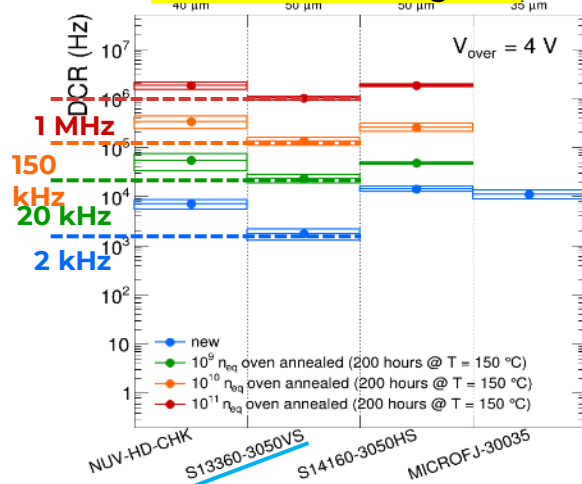
# Results



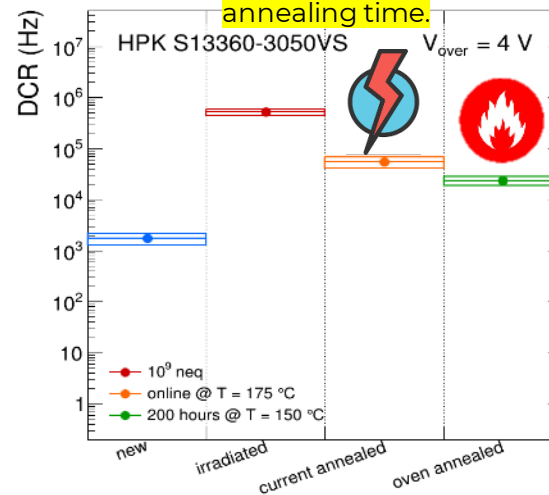
200 hours @ 150°C oven annealing reduces the dark current by a factor  $\approx 100$ .



Hamamatsu S13360-3050 shows less DCR at any irradiation/annealing level



DCR decreases with current annealing without reaching the oven but in 1/10 of the annealing time.



## Conclusions and what's next

SiPMs show to be a good candidate for photon detection in the dRich for EIC.

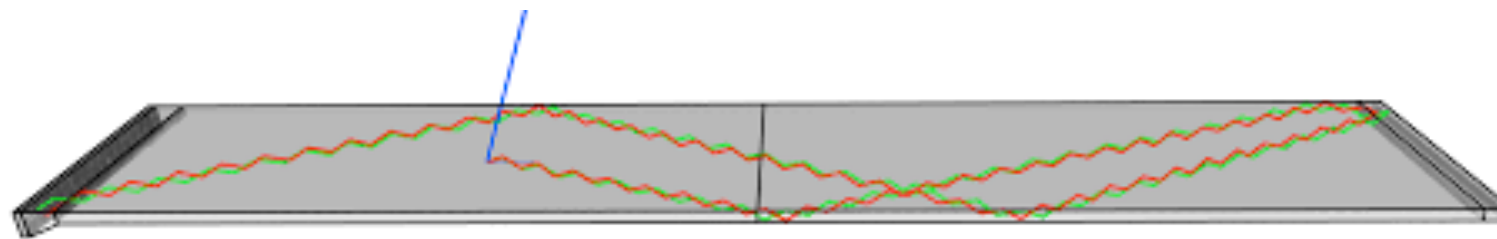
HPK series 13 seems to cope with radiation damage up to  $10^{11}$   $n_{eq}/cm^2$  thanks to the annealing.

Direct current annealing allows in-situ DCR induced by radiation damage reduction.

Neutrons irradiation run at LENA. 3x3cm 256 SiPMs matrix with ALCOR readout and active liquid cooling.

Flavio Dal Corso<sup>(a)</sup>, Roberto Stroili<sup>(a,b)</sup>, Ezio Torassa<sup>(a)</sup>  
 INFN Padova<sup>(a)</sup>, Univ. Padova<sup>(b)</sup>

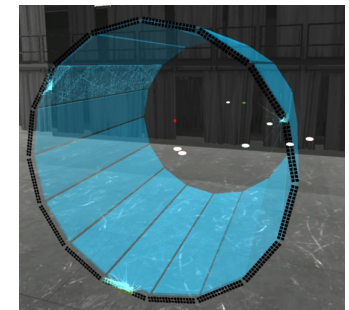
The **T**ime **O**f **P**ropagation is the particle identification detector in the barrel region of the Belle II experiment. The detector uses quartz bars acting as Cherenkov radiators and MCP-PMTs as photodetectors.



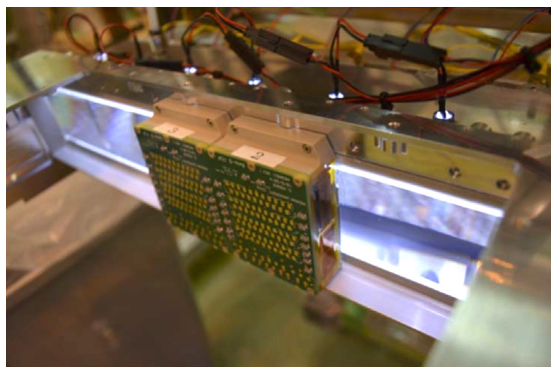
**Quartz Prism**

**Quartz radiator**

**Mirror**



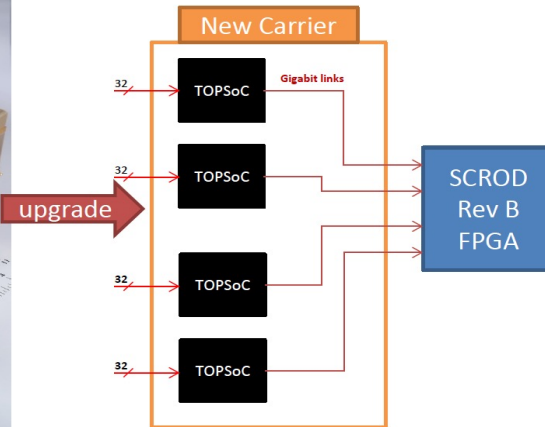
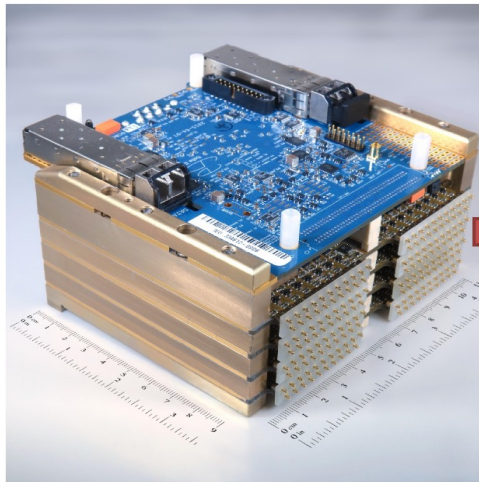
For every TOP module 32 MCP-PMTs 16ch 1 in<sup>2</sup> are optically coupled to the prism



Three generations of MCP-PMT are currently installed in the TOP detector. Long shutdowns of the SuperKEKB accelerator in 2023 and 2027 will be used to upgrade the detector with the last generation of MCP-PMT.

Many improvements in SiPM production technology have been achieved in the last years. Using SiPM as a photodetector is the backup plan for the 2027 upgrade and the primary option for following upgrades with higher luminosity and higher background.

Replacement of MCP-PMT with SiPM will require to upgrade the electronics.

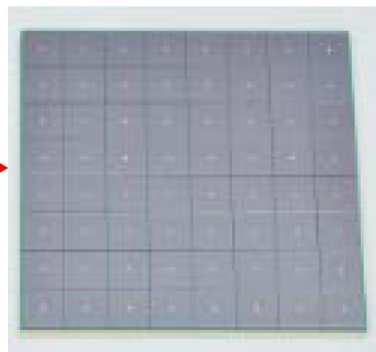


IRSX ASIC 8-channel 250 nm CMOS will be replaced with TOPSoC ASIC 32-channel 130 nm CMOS.

The total number of channels will be increased from 8192 to 32768. Developments of new boards are ongoing at the University of Hawaii

MCP-PMT  
16 ch, 1 in<sup>2</sup>

MPPC (SiPM array)  
64 ch 3x3 mm<sup>2</sup>

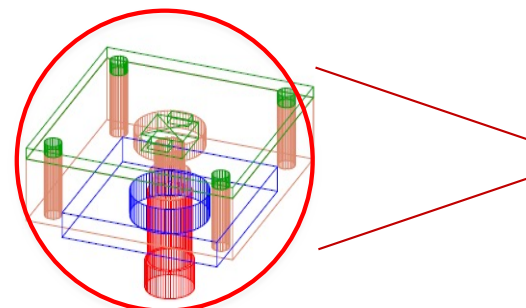
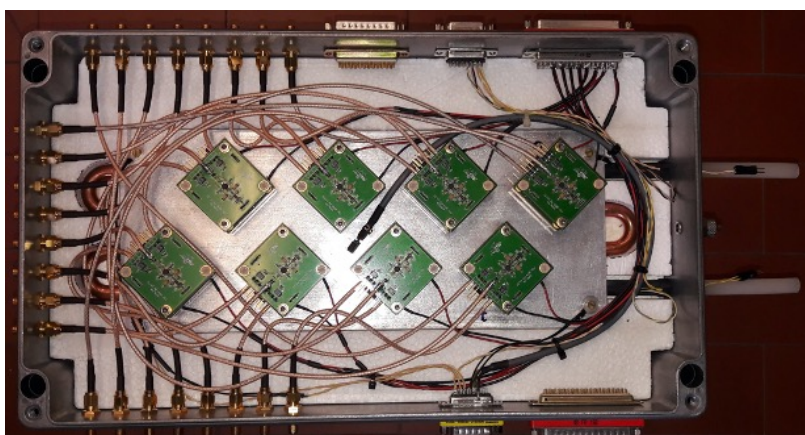


SiPMs compared to MCP-PMTs have higher dark count rate (DCR).

Radiation damages will increase DCR, the effect can be mitigated by lowering the temperature.

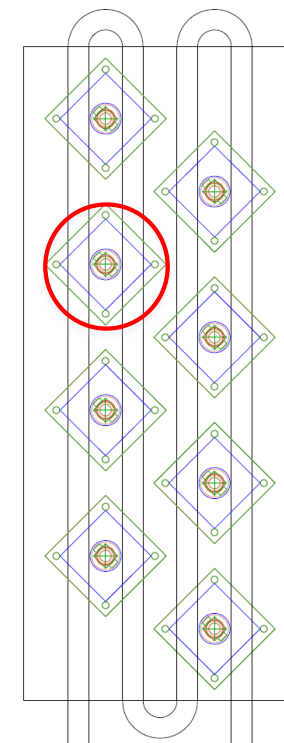
Tests are ongoing in Padova to measure the characteristics of the SiPMs in the market  
 1) for different temperatures 2) before and after irradiation.

Dark box with SiPM blocks



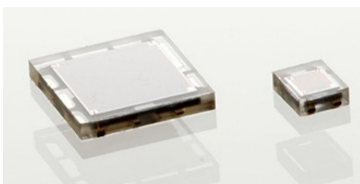
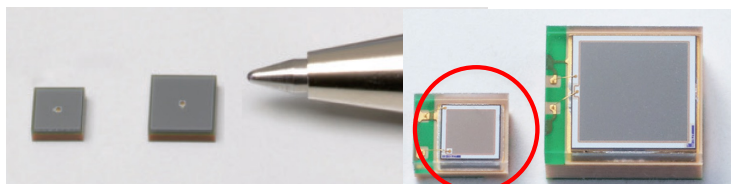

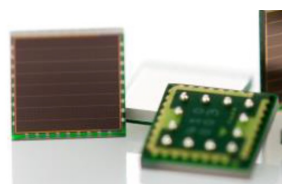
- PCB Amplifier
- PCB SiPM with T sensor
- PCB peltier

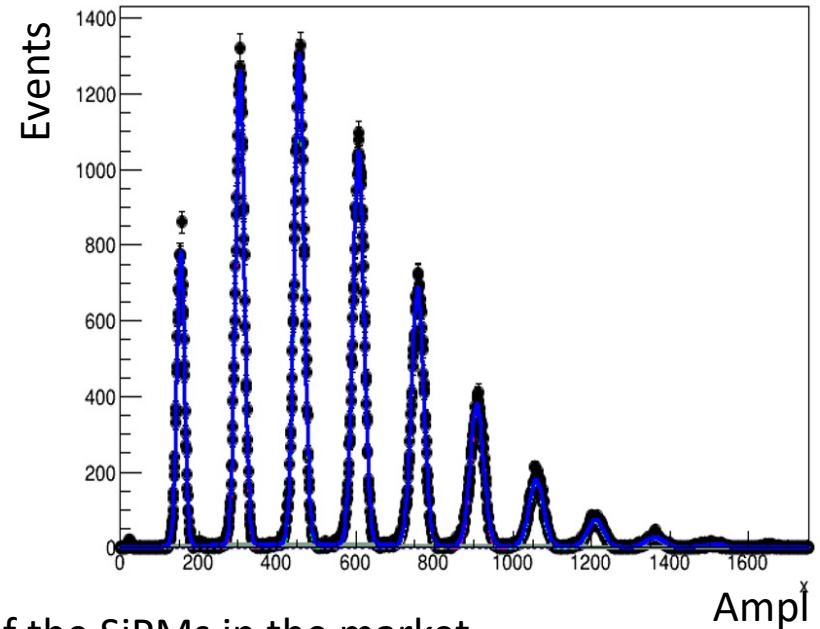
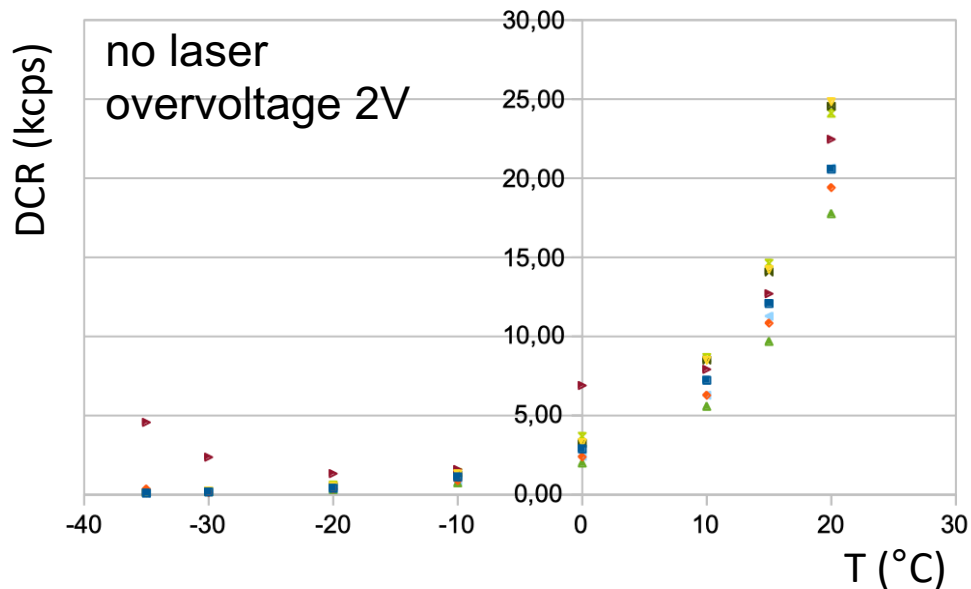
SiPMs illuminated with picosecond laser  
 T from +20 °C to -50 °C



Cooling plate  
 (glycolate water)

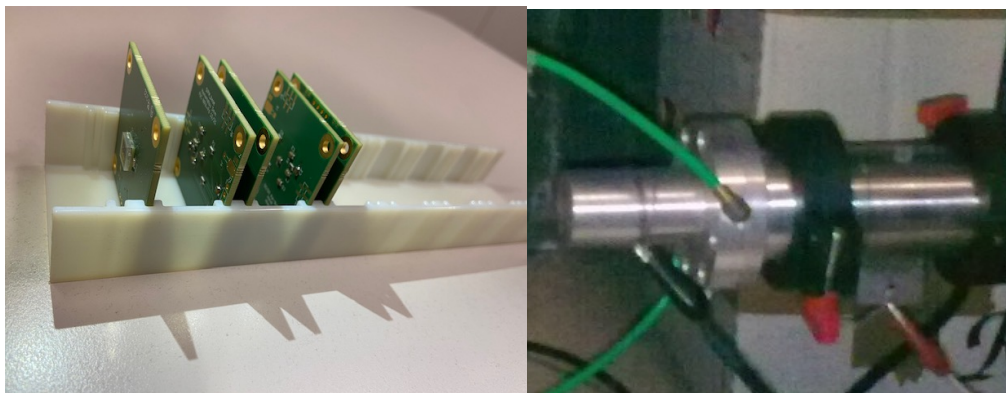
Available SiPMs to be tested

OnSemi (35μm)	Hamamatsu (15-25-50 μm)	FBK (15μm)	Ketek (15-35 μm)
			
1x1 - 3x3 mm <sup>2</sup>	1.3x1.3 - 3x3 mm <sup>2</sup>	1x1 - 3x3 mm <sup>2</sup>	3x3 mm <sup>2</sup>



Tests are ongoing in Padova to measure the characteristics of the SiPMs in the market

1) for different temperatures 2) before and after irradiation.



In November 2022 SiPMs will be irradiated at the LNL CN neutron beam facility with neutron fluxes from  $1 \times 10^{+09}$  to  $5 \times 10^{+11}$  neutrons/cm<sup>2</sup>

SiPM development in collaboration with FBK is inside the AIDAInnova project in the framework of WP 8 task 8.4.1.

Nuova Officina Assergi



a new reality for novel SiPM-based detector production

IFD 2022 : INFN Workshop on Future Detectors  
17-19 October 2022 Bari- Italy



Lucia Consiglio  
INFN LNGS

*Bari Lungomare Rotonda*

# New SiPM technology for light detection

## Why SiPMs?

- Higher Photon Detection Efficiency
- Higher fill factor
- Operated with low bias
- Lower cost

Tile: 24 SiPM array integrated with signal preamplifier  
Photo Detection Module (PDM)

Photo Detection Unit (PDU)

16 tiles -> 4 readout channels

94 900 SPADs

1cm<sup>2</sup>

5 x 5 cm<sup>2</sup>

20 x 20 cm<sup>2</sup>

SPAD: single photon avalanche diode 30 μm pitch

## Challenges

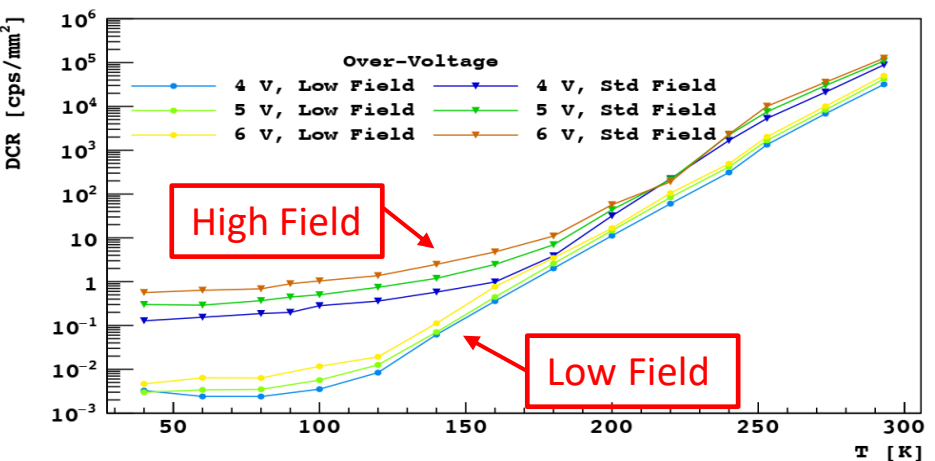
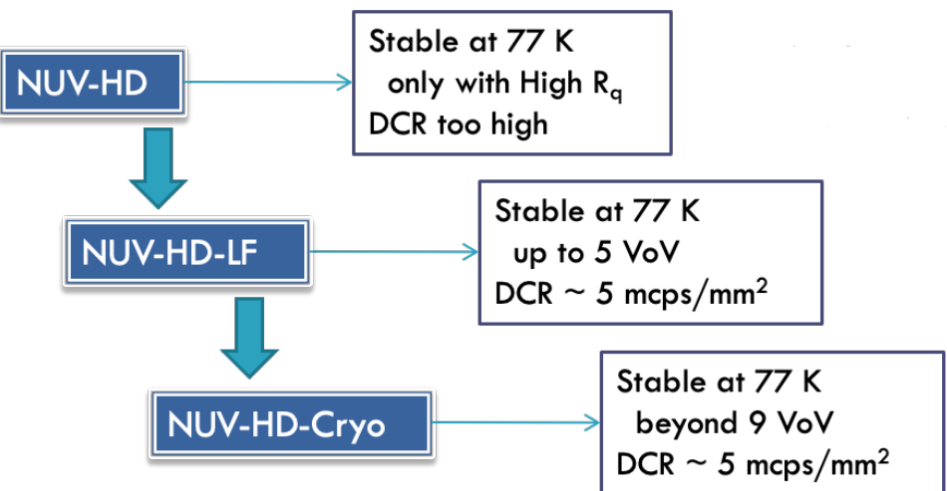
- Large area cryogenic SiPMs
- Low noise cryogenic electronics
- Technological transfer for photosensor massive production

TPC Optical Plane  
21 m<sup>2</sup>

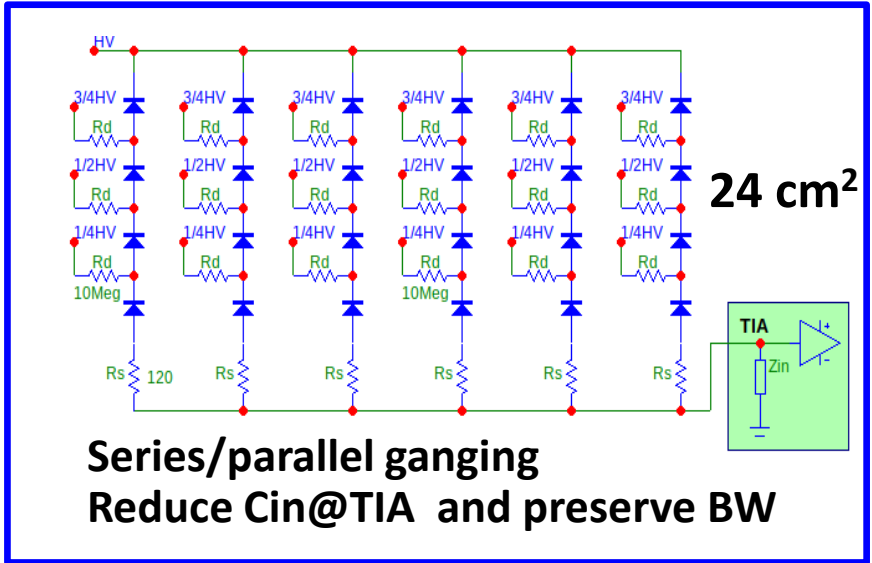
DarkSide-20k top and bottom planes equipped with 528 PDUs

# STEP 1 SiPM development

Custom cryogenic SiPMs developed in collaboration with Fondazione Bruno Kessler (FBK)

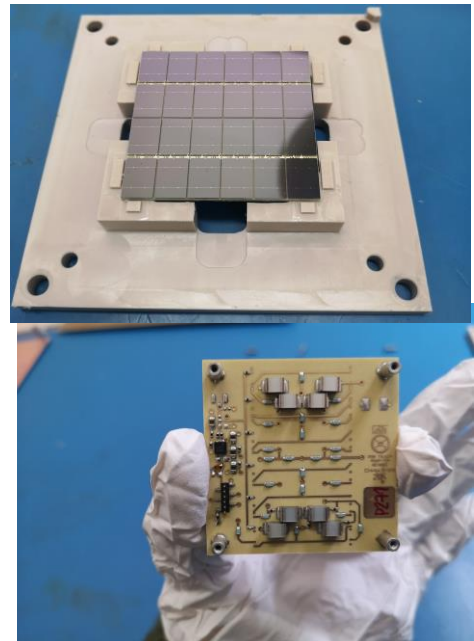


# STEP 2 Electronics design

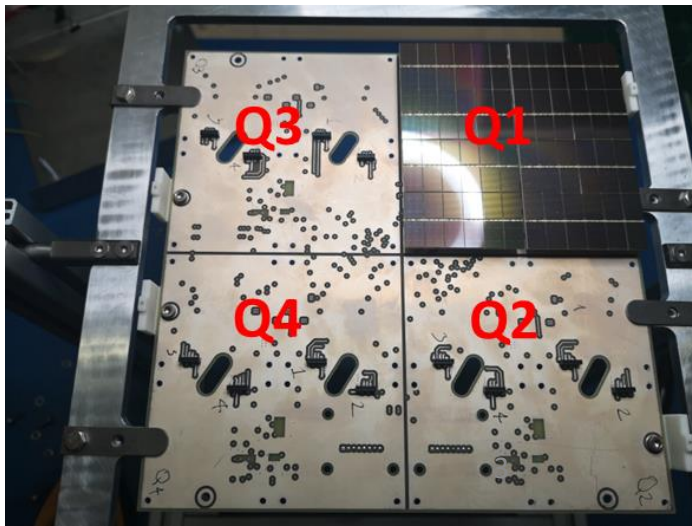


SiPM = current generator + huge output capacitance (~60pF/mm²)  
**Transimpedance amplifier (TIA)**  
**High Bandwidth and Low Noise**

4 PDMs readout as a single analog channel



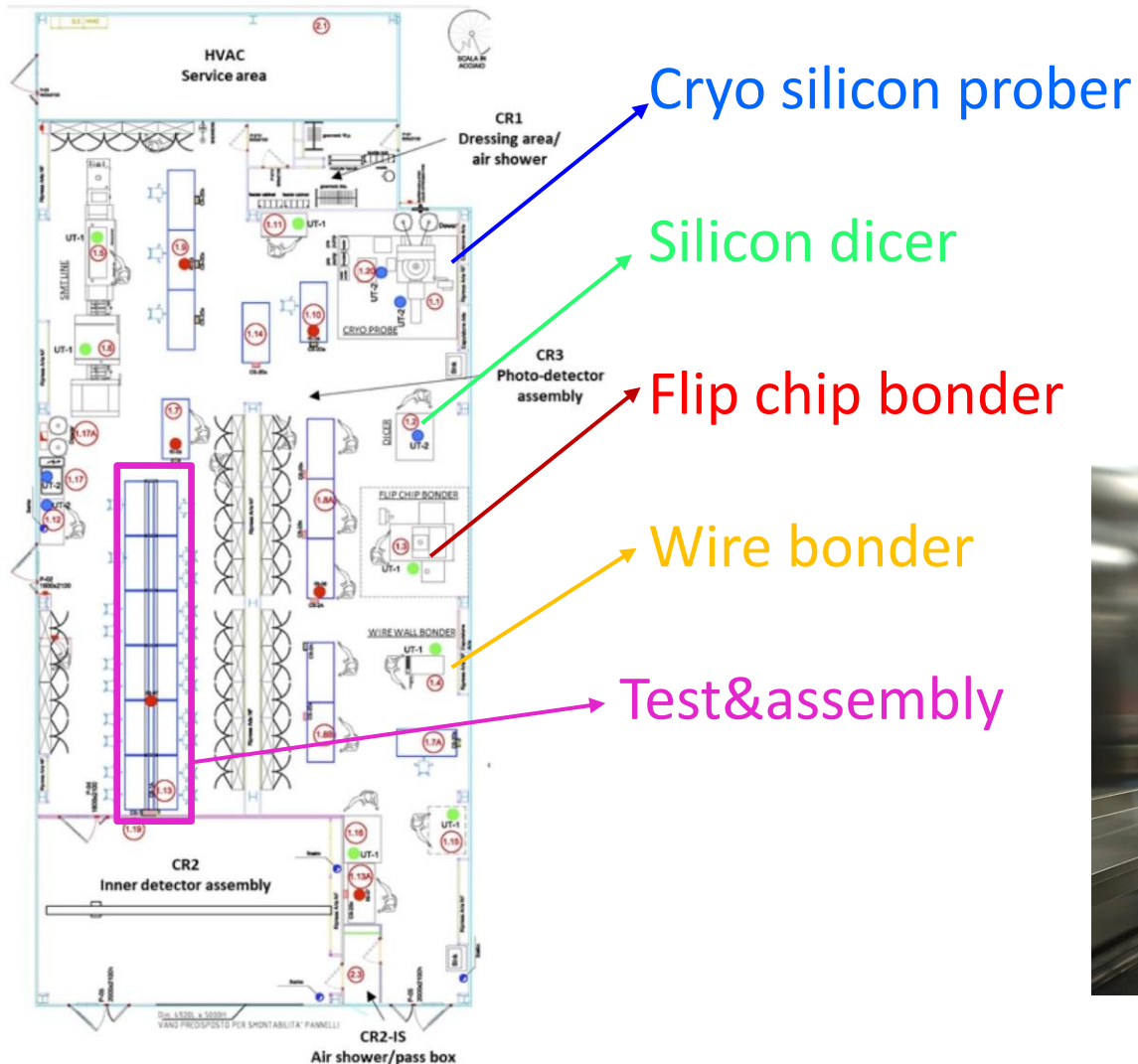
TILE + 1 TIA  
 ↓  
 Photo Detection Module (PDM)





# STEP 3 NOA clean room

420 m<sup>2</sup> clean area in LNGS (PON/RESTART Regione Abruzzo) for packaging, test and assembly of SiPM-based detectors



- Cryoprobe installed and wafer test started.

- Flip chip bonder final installation foreseen by November 2022



# Milestones & perspectives in NOA

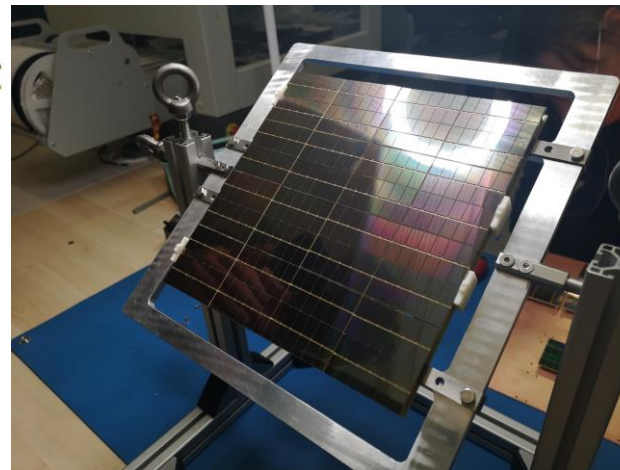
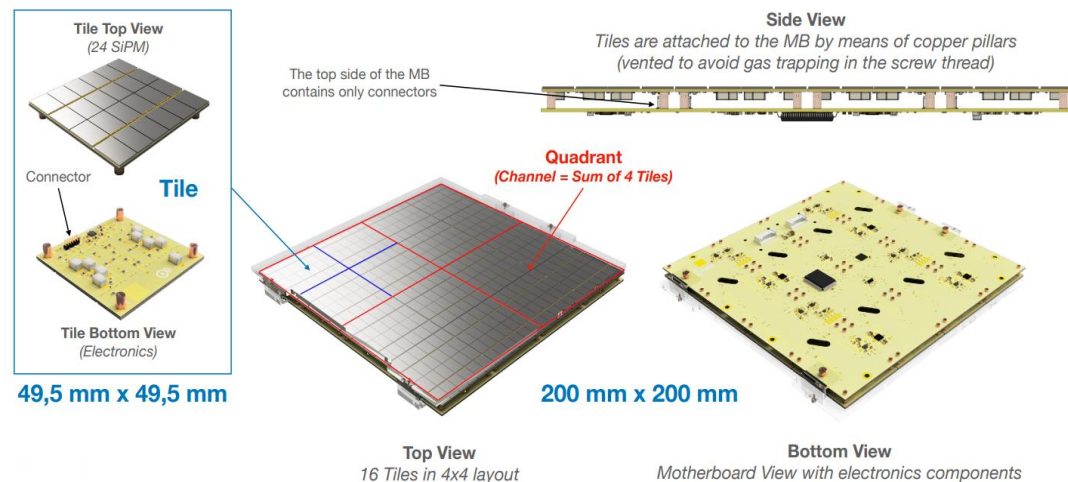
- A unique infrastructure enhancing the high-tech capability INFN LNGS
- Support for integration of large arrays of radiopure SiPM-based photodetectors
- Start up operations in the beginning of 2023

## DarkSide-20k PDU assembly (2023-2025)

## Photo Detection Unit prototype

## What's Next?

- Production and test of photo-detectors for low background experiments.
- Start a network of collaborations to share laboratories and infrastructures



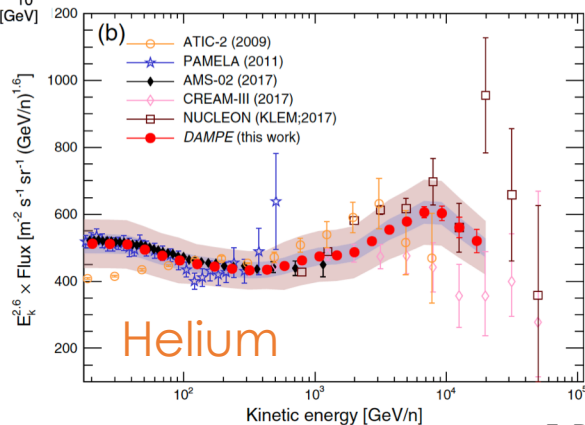
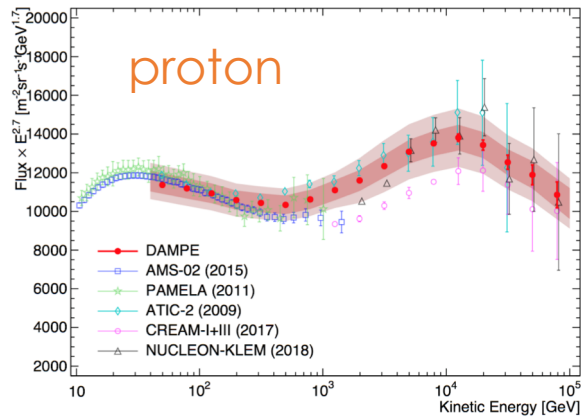
# Particle Identification in Space Experiments with Scintillator Detectors

Felicia Barbato

# Charge Identification of cosmic rays

## Motivation

Identify cosmic rays species to measure the flux and address origin, acceleration and propagation problem



## Plastic scintillator + photosensor



## Principle of operation

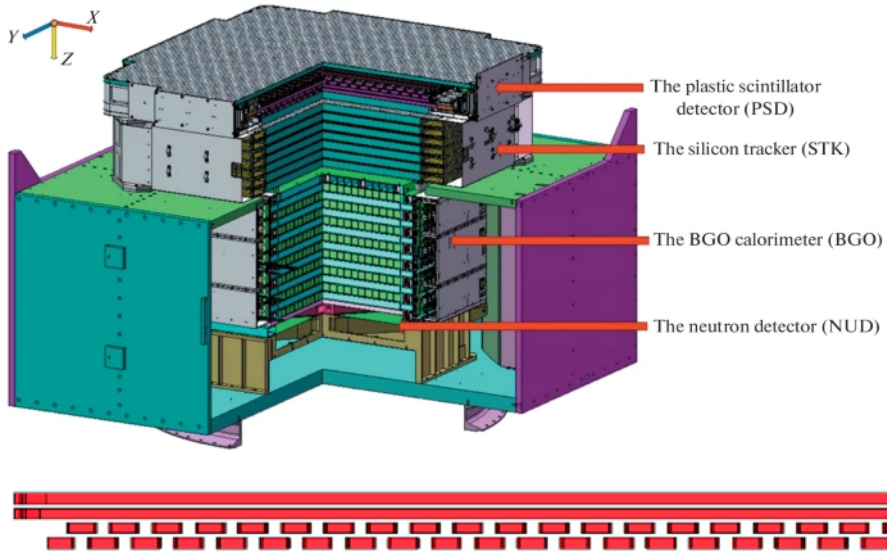
$$-\frac{dE}{dx} = \frac{4\pi e^4 z^2 N Z}{(4\pi\epsilon_0)^2 M_e v^2} \left[ \ln\left(\frac{2M_e v^2}{I}\right) - \ln(1 - \beta^2) - \beta^2 \right]$$

Bethe Bloch formula

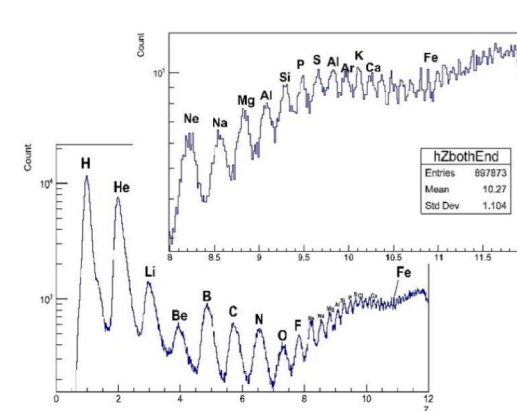
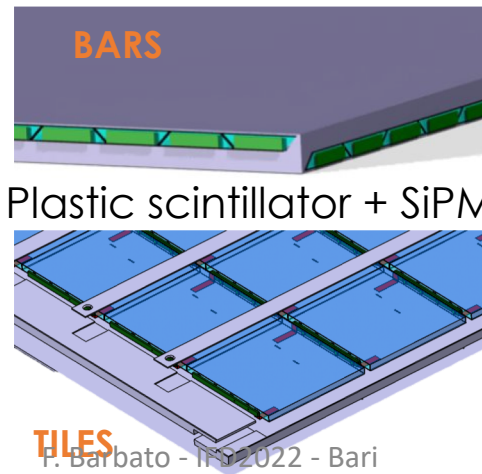
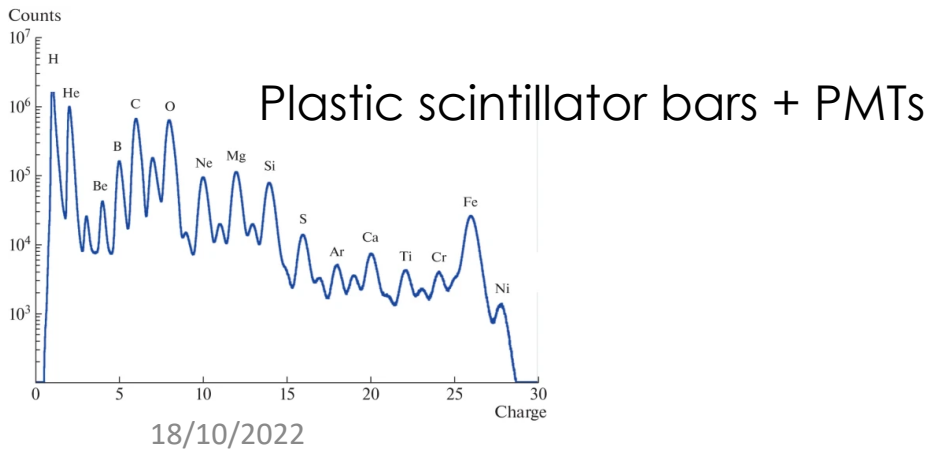
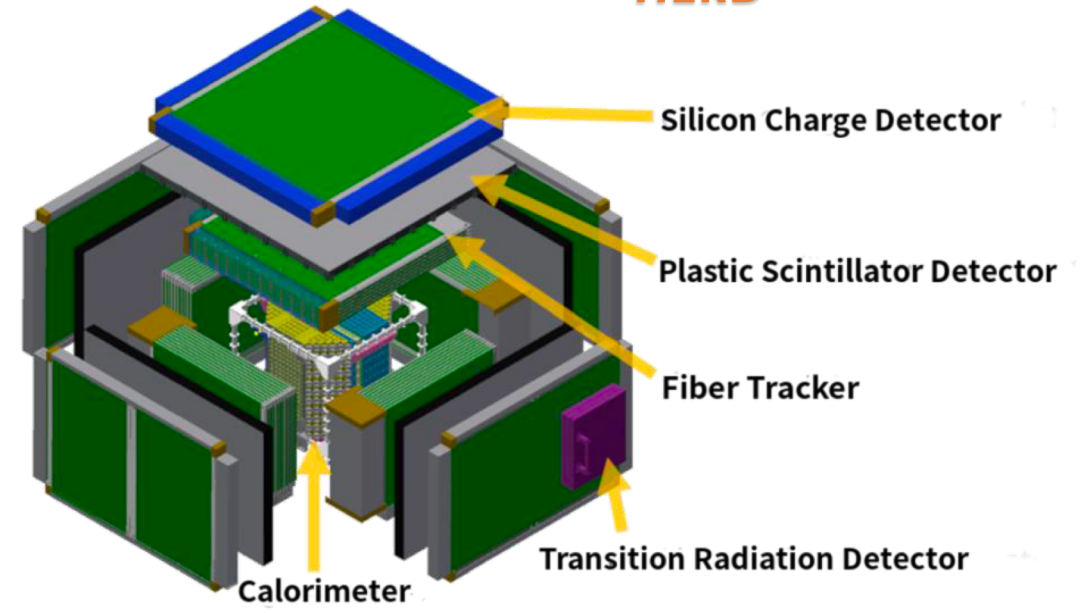
Ionization energy loss of charged particles

# Plastic Scintillator Detector

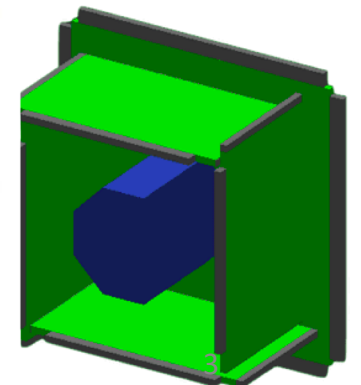
## DAMPE



## HERD

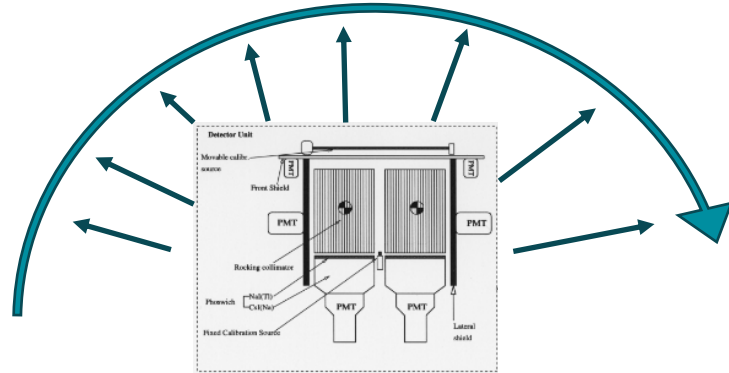


High hermeticity



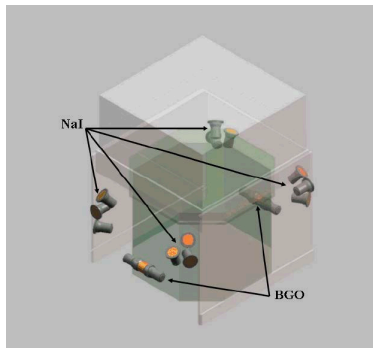
# Gamma-ray identification

## Beppo-Sax



- Phoswich technique with collimators
- Orientable mechanics
- One module

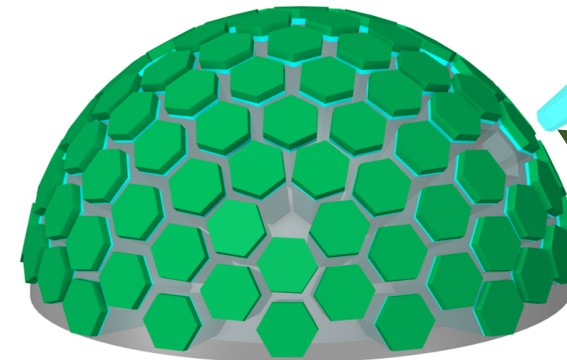
## Fermi-GBM



- Triangulation over 12 pixel ( $\varnothing$  12.7 cm)
- Different orientation
- One module

## Crystal Eye

VETO  
Charged particles

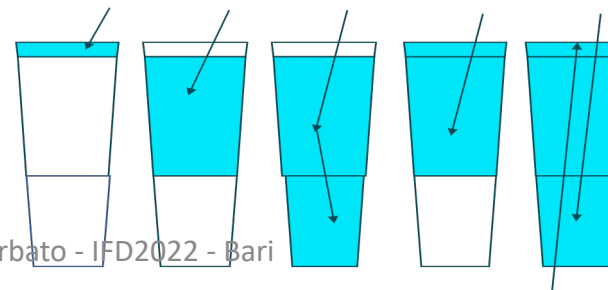


UP-PIXEL  
 $E_\gamma < 1\text{MeV}$

SiPM ARRAY  
4x4

DOWN-PIXEL  
 $E_\gamma > 1\text{MeV}$

- Charge distribution over 112 pixel ( $\varnothing \sim 5\text{cm}$ )
- Compact photosensors (simplified phoswich, no need for pulse shape discrimination)
- Compact hemispherical design (no need for orientable mechanics)

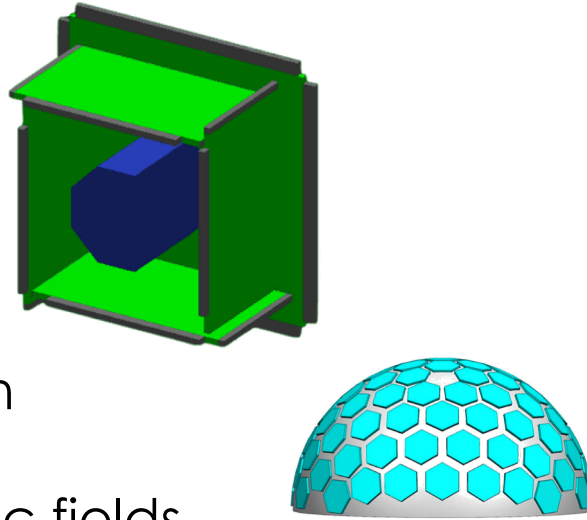


- a – Down-going hard X-ray
- b – Down-going LE g-ray
- c – Down-going ME g-ray
- d – Down-going LE charged particle
- e – HE charged particle

# Scintillators + SiPMs

## PROS

- Compact design
- Low power consumption
- Easy redundancy
- No sensitivity to magnetic fields



## CONS

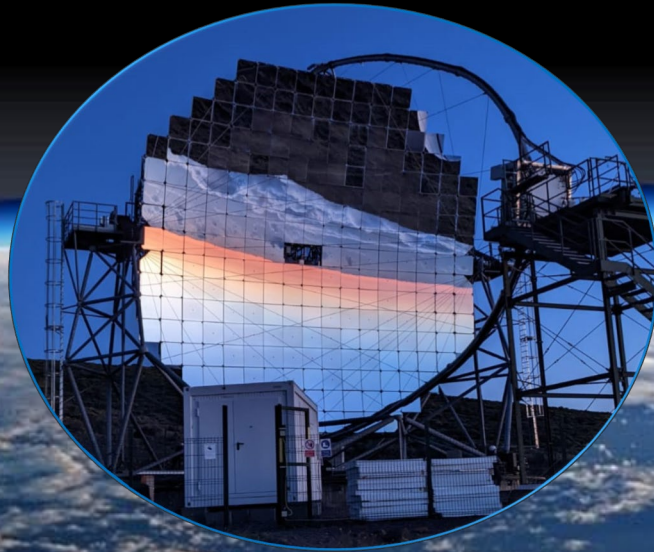
- Non space qualified
  - packaging issue
  - radiation damage
- high dcr

**OPEN DISCUSSION ABOUT FUTURE**

# Gamma-ray identification with Imaging Atmospheric Cherenkov Telescopes

Di Venere Leonardo

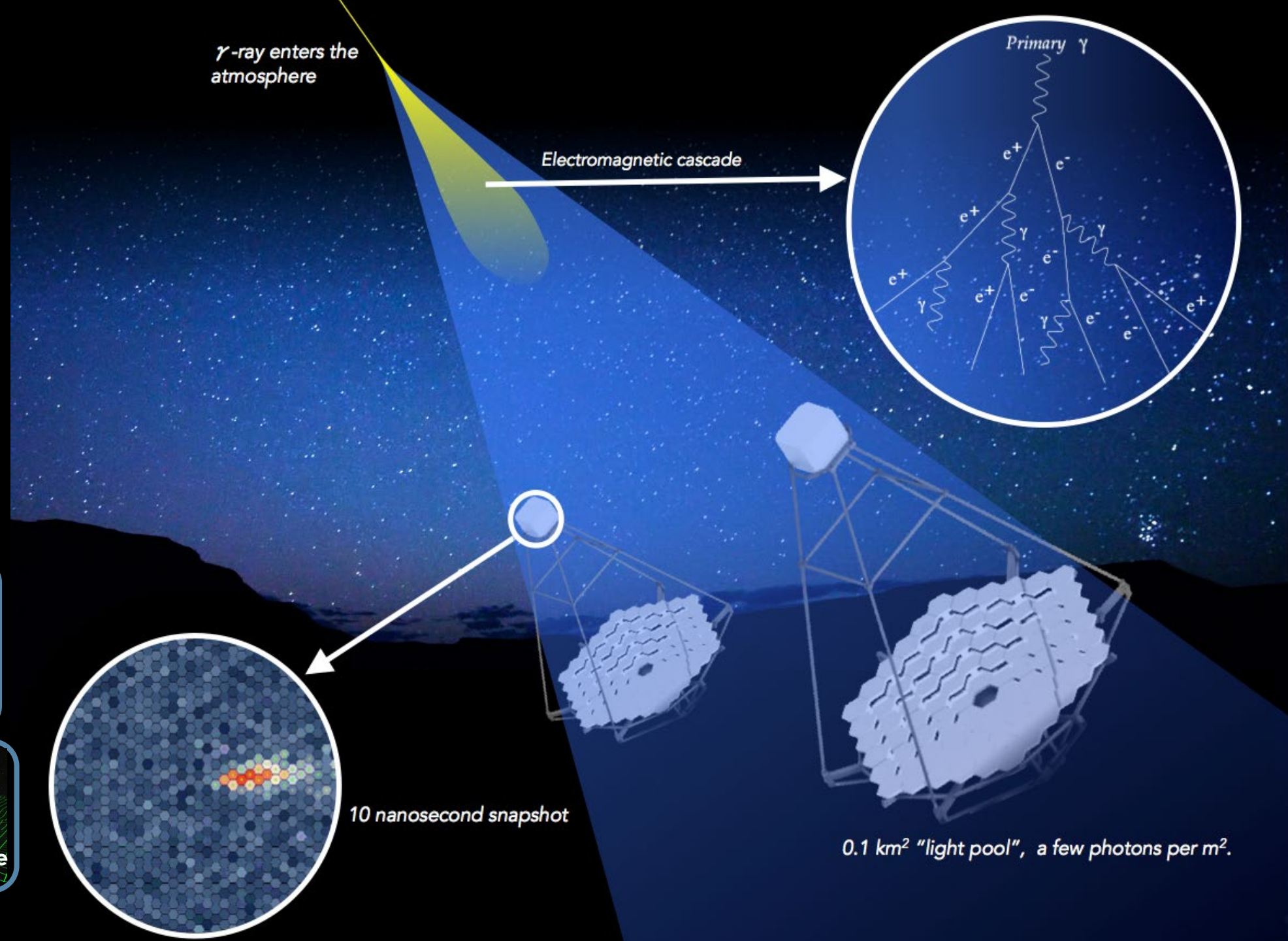
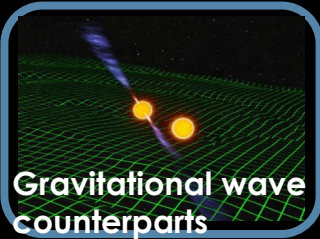
Università e INFN Bari  
[leonardo.divenere@ba.infn.it](mailto:leonardo.divenere@ba.infn.it)





# Imaging Atmospheric Cherenkov Telescopes

TeV gamma-ray ideal to probe the most energetic Universe



# Particle identification

- Gamma rays and cosmic rays produce particle showers in atmosphere which emit Cherenkov light
- Shower images detected by fast high-resolution cameras
- ML algorithms used for the particle identification and the measurement of direction and energy of the primary particle

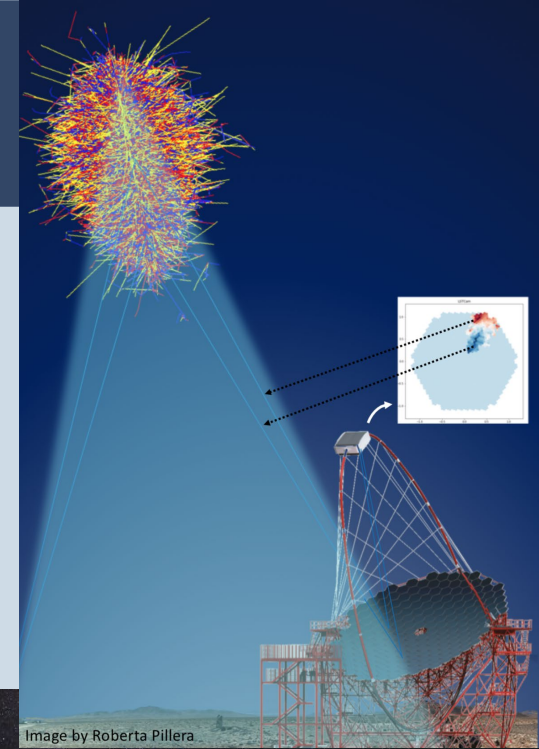
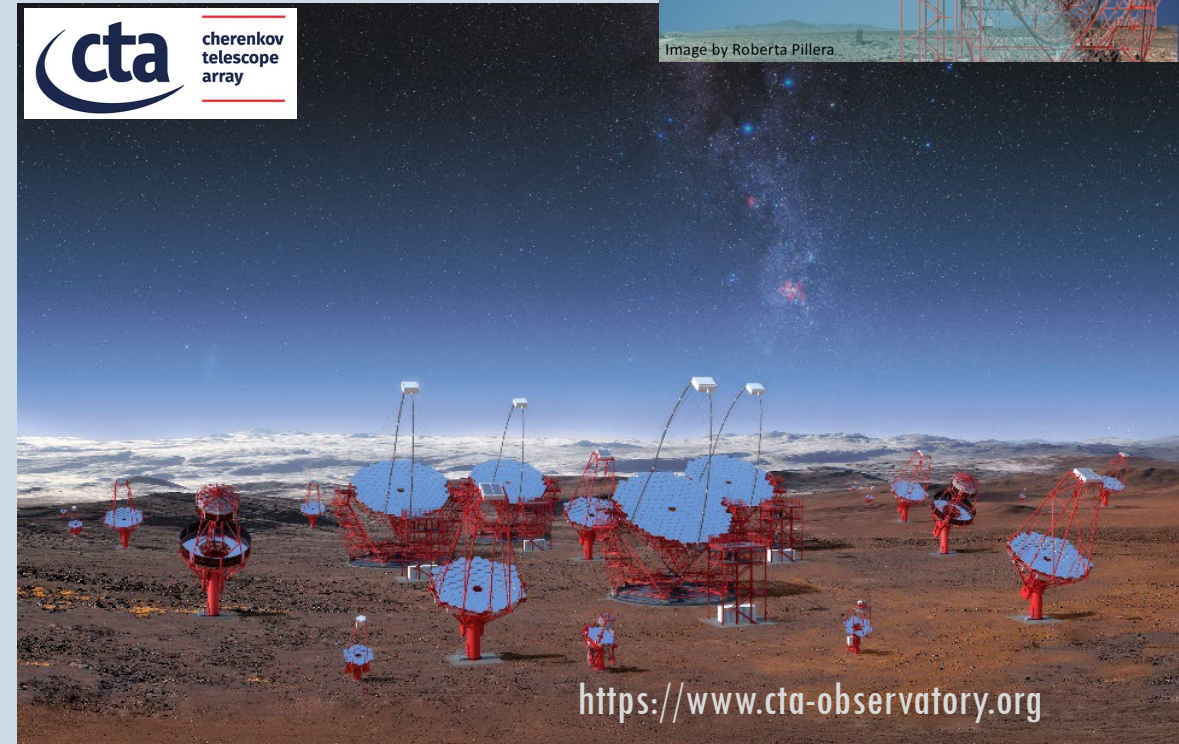
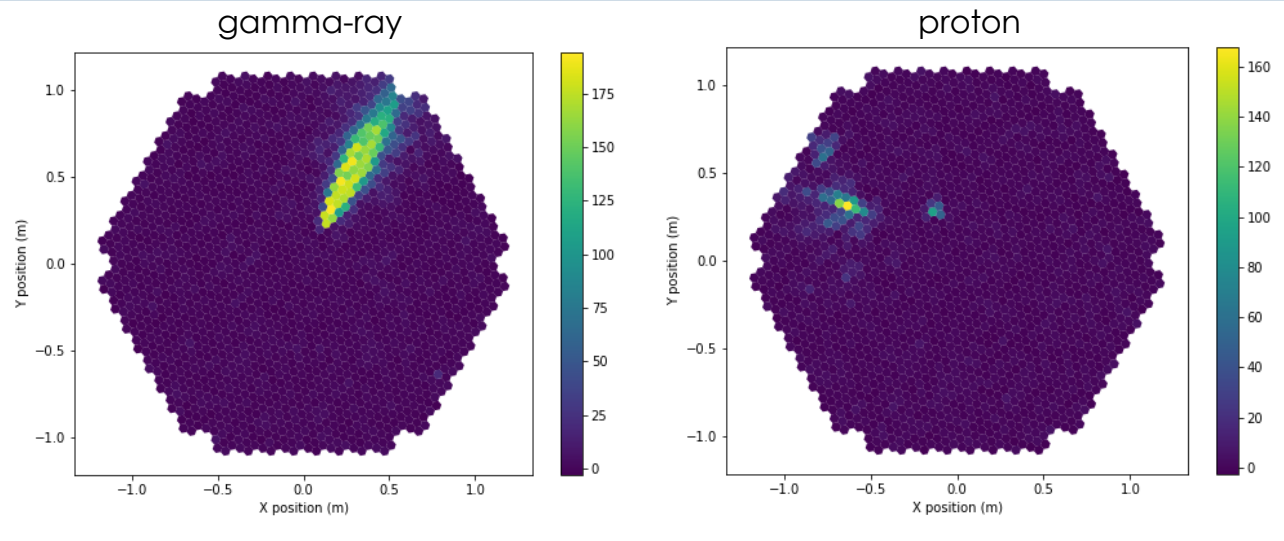


Image by Roberta Pillera



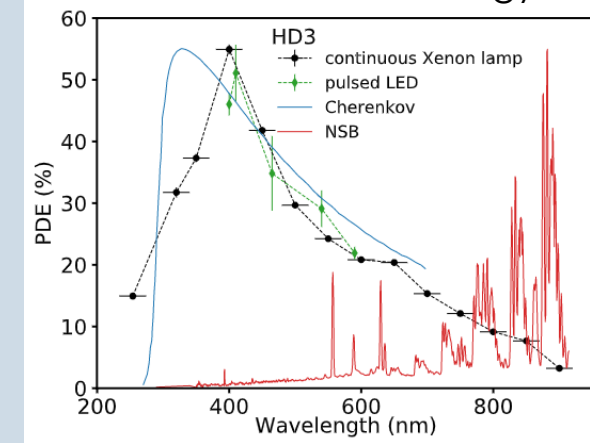
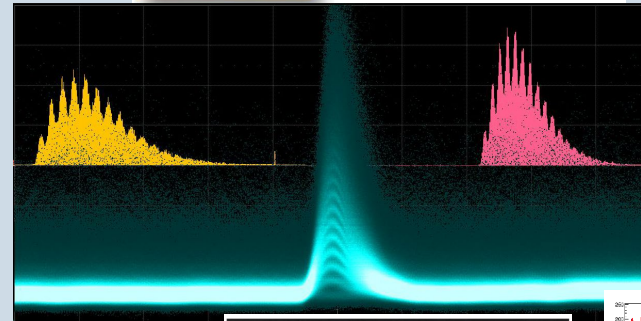
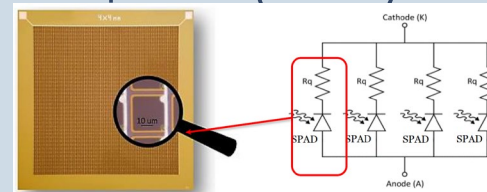
# IACT camera

- Need to detect faint (down to few p.e.) and fast ( $\sim$ tens of ns) Cherekov light
- Need to deal with night sky background (NSB) light
- Photon detectors: Photomultiplier Tubes (PMT)  $\rightarrow$  Silicon Photomultipliers (SiPM)
- Pros:
  - Single p.e. resolution
  - NSB tolerant  $\rightarrow$  Operable under full moon
  - High PDE ( $> 50\%$  peak)
  - Small pixels  $\rightarrow$  easy to make arrays
  - Low bias voltage ( $< 100V$ )
- Cons:
  - High sensitivity to NSB in  $> 550$  nm range
  - Correlated noise
  - high dark count rate  $\rightarrow$  usually below the NSB rate

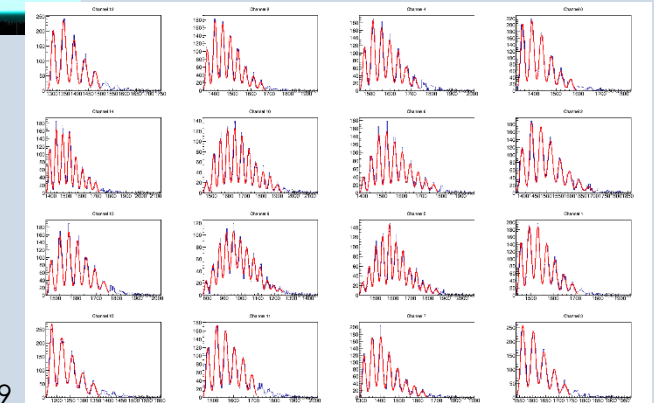
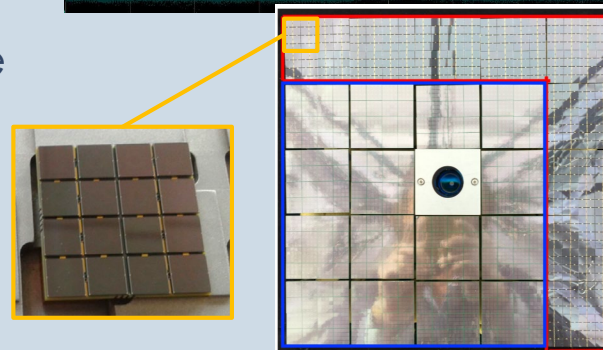


pSCT@FLWO

FBK NUV-HD technology



Ambrosi+2022 Submitted to NIMA

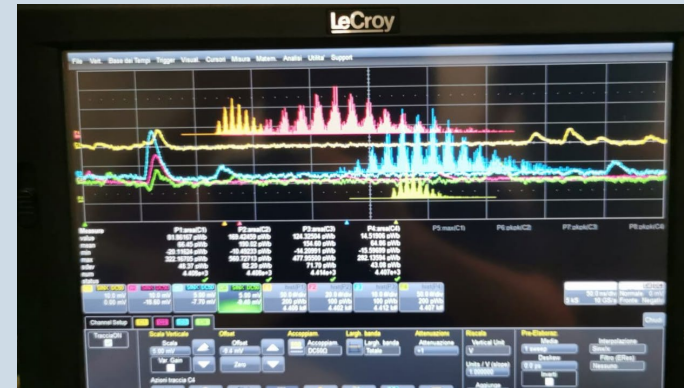
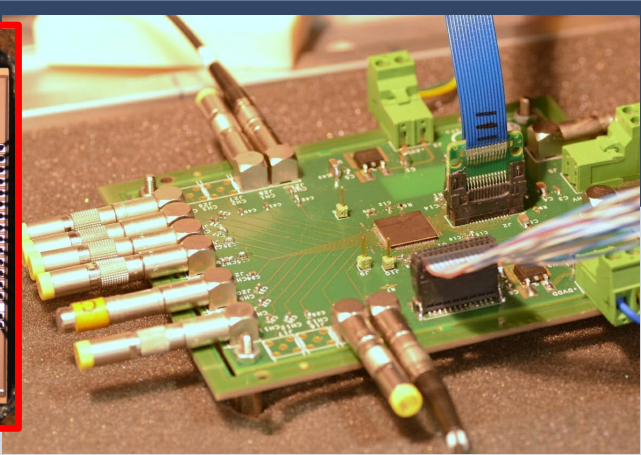
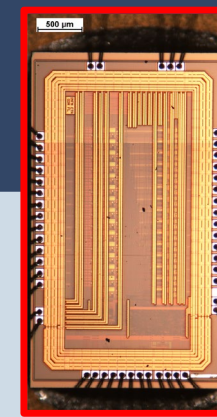


# Fast and single p.e. resolution frontend electronics

**SMART:** a SiPM Multichannel Asic for high Resolution Cherenkov Telescopes

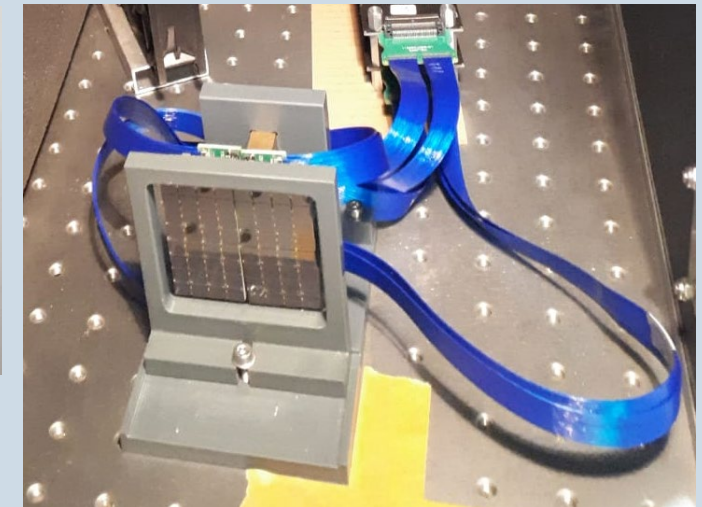
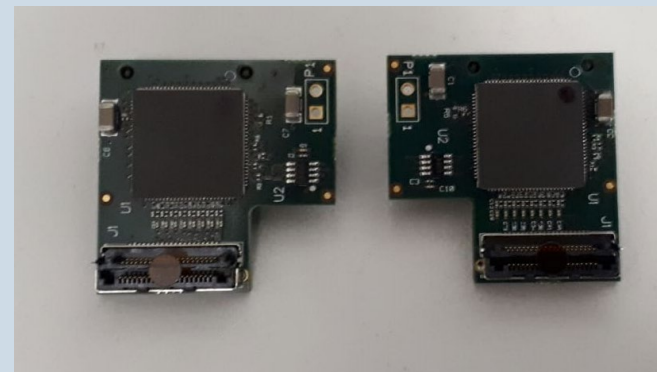
## Features:

- 16-channel trans-impedance amplifier
- Fast path gain: 1-3 mV/ph
- Tail suppression: pulse duration  $\sim 10$ ns
- Power consumption: 20mW/channel
- SiPM bias fine tuning: LSB = 12.5mV
- Slow path output & 10 bit ADC: LSB = 2MHz
- Output dynamic range:
  - 900 mV without external PZ
  - 600 mV with external PZ
- $\sim 800$  ASICs tested @INFN Bari

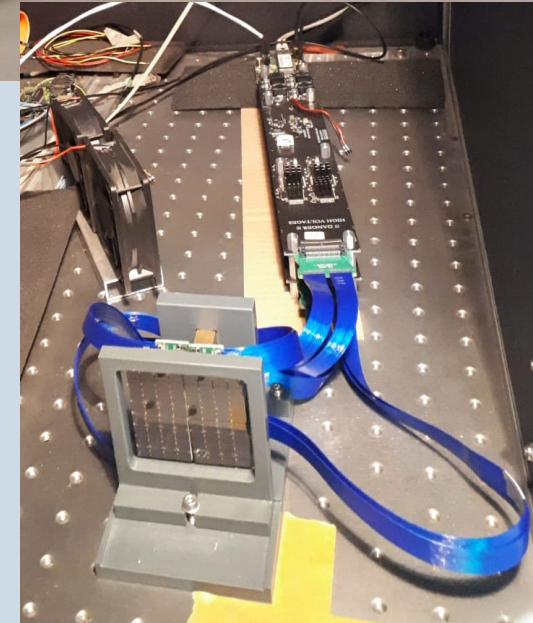
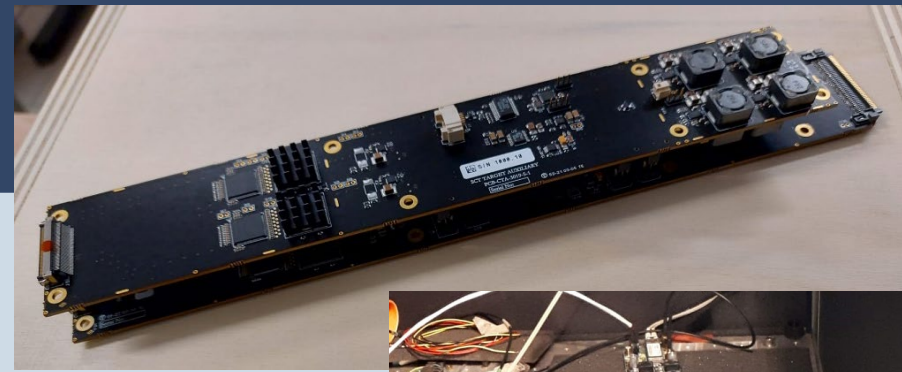


Designed by F. Licciulli & G. De Robertis at the Electronics CAD INFN Bari

Contact:  
[francesco.licciulli@ba.infn.it](mailto:francesco.licciulli@ba.infn.it)



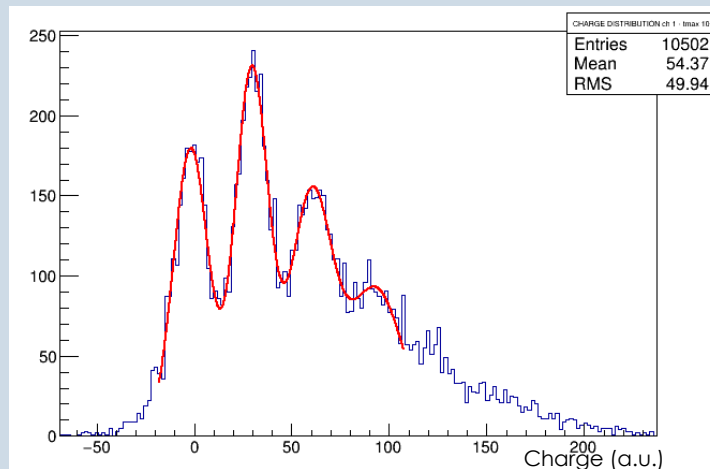
# Readout electronics



Readout electronics to digitize fast signals and generate trigger signals at pixel level → TARGET ASICs

- CTC ASIC: 16-channel 1GSa/s digitizer
  - Analog buffer with 16k cells per channel → 16 us storage depth
- CT5TEA ASIC: 16-channel trigger ASIC
  - Channels are summed in groups of 4 to obtain 4 trigger pixels per ASIC

Single p.e. spectrum



Rate scan

